Energy Conversion and Management 288 (2023) 117130

Contents lists available at ScienceDirect

Energy Conversion and Management

journal homepage: www.elsevier.com/locate/enconman

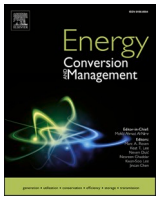

Energy, exergy, exergoeconomic, and exergoenvironmental (4E) analysis of a new bio-waste driven multigeneration system for power, heating, hydrogen, and freshwater production: Modeling and a case study in Izmir

Zahra Hajimohammadi Tabriz [a], Mousa Mohammadpourfard [a,b,*], Gülden Gökçen Akkurt [b], Saeed Zeinali Heris [a]

[a] Faculty of Chemical and Petroleum Engineering, University of Tabriz, Tabriz, Iran
[b] Department of Energy Systems Engineering, Izmir Institute of Technology, Izmir, Türkiye

ARTICLE INFO

Keywords:
Multigeneration system
Exergy
Hydrogen
Atmospheric water harvesting
Sewage sludge Biomass
4E analysis

ABSTRACT

Today, the world is facing numerous challenges such as the increasing demand for energy, fossil fuels reduction, the growth of atmospheric pollutants, and the water crisis. In the present research, a new multigeneration system based on urban sewage bio-waste has been designed and evaluated for power, hydrogen, freshwater, and heating production. This system, which consists of biomass conversion subsystem, hydrogen production unit, Brayton cycle, atmospheric water harvesting unit, steam Rankine cycle, and organic Rankine cycles, has been evaluated from a thermodynamic point of view, and the energy, exergy, exergoeconomic, and exergoenvironmental analyses have been carried out on it. In the current study, the atmospheric water harvesting unit, as an attractive and environmentally friendly technology, is integrated with this Biomass-based multigeneration. A case study has been conducted on this system using the information collected from Çiğli wastewater treatment plant located In Izmir province, Turkey, and the results indicate that such a system, in addition to receiving sewage sludge from the treatment plant unit as a polluting waste, can produce added value products. The modeling results show that in the base conditions and with a feed rate of 7.52 kg/s, the total power generated by this system is 17750 kW, the hydrogen production rate is 3180 kg/h, the freshwater production rate is more than 18 l/h, and the energy and exergy efficiencies are 35.48% and 40.18%, respectively. According to the exergoeconomic and exergoenvironmental evaluations, the unit cost of total products and the unit emission of carbon dioxide are calculated as 13.05 $/GJ and 0.2327 t/MWh, respectively. Also, the results of parametric studies show that increasing the rate of Biomass improves the overall energy efficiency and production rates and also reduces the unit emission of carbon dioxide, but on the other hand, it causes a decrease in exergy efficiency and an increase in the unit cost of total products.

1. Introduction

Nowadays, the world's most important concerns are energy, environment, and water. The increase in energy demand, the reduction of fossil fuels, and the low efficiency of traditional power plants are the challenges in the energy field. In the last ten years, the world's energy demand has increased by 1.7% annually [1]. However, traditional power plants have only 30% fuel-to-electricity efficiency [2]. Burning fossil fuels and even some procedures for clean fuel production have caused environmental effects, greenhouse gas emissions, and global warming. According to the International Energy Agency (IEA) reports, the current primary energy supply is more than 12×10^9 tons of oil equivalent, which causes the emission of 39.5 Gt of CO_2 [3]. Moreover, the asymmetric distribution of water all over the world and the lack of available freshwater have caused water stress in many parts of the world. Although 70% of our planet is covered with water, only 2.5% of this water is available as freshwater. About 4×10^9 people experience water shortage for at least one month a year, and about 5×10^8 people face this issue all year long [4,5].

Designing and evaluating polygeneration systems is a promising solution to reduce energy issues. Polygeneration systems simultaneously produce two or more than two energy products in a single integrated process [6]. The design of polygeneration systems enhances efficiency

* Corresponding author at: Department of Energy Systems Engineering, Izmir Institute of Technology, İzmir / Türkiye.
E-mail addresses: mohammadpour@tabrizu.ac.ir, mousamohammadpourfard@iyte.edu.tr (M. Mohammadpourfard).

https://doi.org/10.1016/j.enconman.2023.117130
Received 2 January 2023; Received in revised form 29 March 2023; Accepted 30 April 2023
Available online 11 May 2023

Nomenclature

ARC	Absorption refrigeration cycle
AWH	Atmospheric water harvesting
BC	Brayton cycle
BCS	Biomass conversion system
$c(\$/GJ)$	Specified cost per unit of exergy
$\dot{C}(\$/s)$	Cost rate
$c_p(\$/GJ)$	Unit cost of product
$C_{ei}(-)$	Exergoenvironmental impact coefficient
CEPCI	Chemical Engineering Plant Cost Index
CEHX	Condenser–evaporator heat exchanger
COP	Coefficient of performance
$CRF(-)$	Capital recovery factor
Des	Destruction
$E(kJ)$	Energy
$EMI_{CO_2}(t/MWh)$	Unit emission of carbon dioxide
$ex(kJ/kg)$	Special exergy
$f_{ei}(-)$	Exergoenvironment factor
$f_{es}(-)$	Exergy stability factor
$f_k(-)$	Exergoeconomic factor
$\bar{g}(kJ/kmol)$	Molar specific Gibbs free energy
$h(kJ/kg)$	Specific enthalpy
$\bar{h}(kJ/kmol)$	Molar specific enthalpy
$\bar{h}_f^0(kJ/kg)$	Molar specific enthalpy of formation
$i(-)$	Interest rate
K(-)	Equilibrium constant
$\overline{LHV}(kJ/kmol)$	Molar lower heating value
$\dot{m}(kg/s)$	Mass flow rate
MC(-)	Moisture content
$MW(kg/kmol)$	Molar weight
$N(h)$	Annual duration of operation hours
$n(Year)$	Lifetime of the project
ORC	Organic Rankine cycle
$\dot{Q}(kJ/s)$	Heat transfer rate
$R(kJ/kg)$	Universal gas constant
$\bar{R}(kJ/kmol.K)$	Universal molar gas constant
$s(kJ/kg.K)$	Specific entropy
$\bar{s}(kJ/kmol.K)$	Molar specific entropy
SHX	Solution heat exchanger
SRC	Steam Rankine cycle
$STBM$(-)	Steam to Biomass ratio
RH (-)	Relative humidity
$t(s)$	Time
$TPC(kJ/s)$	Total power consumption
VS(-)	Volatile solid
$\dot{W}(kJ/s)$	Power
WGR	Water generation rate
WGSRU	Water-gas shift reaction unit
WWTP	Wastewater treatment plant
$x(kg/kg_{solution})$	Ammonia mass fraction
y	Exergy destruction ratio
$Z_k(\$)$	The cost of k_{th} component
$\dot{Z}(\$/s)$	Capital investment cost

Greek letters

ε	Heat exchanger effectiveness
η	Energy efficiency
θ_{ei}	Environmental damage effectiveness factor
θ_{eii}	Exergoenvironmental impact improvement
$\bar{\lambda}$	Fuel-air ratio on the molar basis
ϕ	Maintenance factor
ψ	Exergy efficiency
ω	Specific humidity
$\tilde{\omega}$	Vapor mole fraction ratio

Subscripts and superscripts

0	Standard conditions
a	Air
ch	Chemical
cv	Control volume
D	Destruction
DA	Dry air
DS	Dry solid
e	Exit
ha	Relative humidity
i	Input
mix	Mixture
OM	Organic matter
ph	Physical
w	Water

and reduces pollution by utilizing waste energy or stream of the system in other subsystems [7].

The energy used in these plants can be supplied through fossil fuels, but due to their disadvantages in causing pollution, researchers tend to replace them with cleaner fuels. Using cleaner and more affordable fuels such as shale gas [8] in multigeneration systems or co-firing Biomass with fossil fuels [9] has been the subject of recent studies in this field. Renewable energy sources, as the most important and clean energy sources, when used in polygeneration systems, combine the benefits of using renewable energy sources with those of polygeneration. The integration of solar energy [10], geothermal energy [11], and Biomass energy [12] with multigeneration systems has been the most popular topic in recent studies.

Unlike other renewable energy sources, Biomass has no intermittent nature and has gained much popularity due to its easy storage, high availability, and carbon neutrality [13]. In addition, the use of wasted Biomass (Bio-waste) has an additional advantage because it does not chiefly compete with the food chain or other benefits [14]. Municipal sewage sludge is one of the most important types of Bio-waste. A large amount of sewage sludge is produced from municipal wastewater treatment plants around the world. Sludge production is continuously increasing and it is predicted that its amount, which is currently around 50 g of dry matter per person per day, will not decrease in the future. The implementation of municipal sewage sludge, as the feed of polygeneration systems is a suitable solution to produce valuable products from a polluting waste [15]. Power and heating are typical products of Biomass-based plants. Also, the coupling of hydrogen production processes with these systems has received a lot of attention. Hydrogen is known as a clean fuel that does not cause harmful emissions when used to generate electricity. But one thing to note is that clean fuel is important when its overall life cycle is environmentally benign. Hydrogen production using renewable energy sources or through the Biomass conversion cycles is a promising solution [16].

Ishaq et al. [17] proposed a Biomass driven system for power, hydrogen, heating, and hot water production. This system uses low-grade waste heat for organic Rankine cycle and the thermoelectric generator. The overall energy efficiency is obtained to be 50.83%, whereas the exergy efficiency is found to be 32.78%. In another study, Ishaq et al. [18] designed a Biomass driven plant to produce power, heating, and hydrogen. The hydrogen is produced in a PEM electrolyzer and water gas shift reactor. They showed that energy and exergy efficiencies are 53.7% and 45.5%, respectively. Sotoodeh et al. [19]

developed a waste-to-energy Biomass gasification-based multigeneration system that produces power, heating, cooling, and hydrogen. They have improved power generation in the cycle by 12%. Energy and exergy analysis and a comprehensive parametric study on the cycle have been done, and the energy and exergy efficiencies obtained 52.3% and 41.3%, respectively.

Water stress, as mentioned earlier, is a problem that threatens the coming decades of the planet. Therefore, integrating water desalination units with energy systems to simultaneously produce freshwater and other products is also considered. In the system proposed by Safari et al. [14], a sewage sludge bio-waste-based multigeneration system was developed to produce electricity, heating, freshwater, and hydrogen. The main subsystems of this plant are a Brayton cycle fueled with biogas from anaerobic digestion, a multi-effect desalination unit, and an organic Rankine cycle. This system's energy and exergy efficiencies are 63% and 40%, respectively. Yilmaz et al. [20] designed a system based on demolition wood that produces electricity, heating, freshwater, and hydrogen. This system uses a membrane distillation unit to produce freshwater. Furthermore, the produced hydrogen is obtained from the high-temperature steam electrolyzer subsystem. This system's energy and exergy efficiencies are reported as 52.84% and 46.59%, respectively. Onder et al. [21] proposed a system for producing electricity, heating, cooling, hydrogen, hot water, and drying. Hydrogen production in this system is through a four-step Cu-Cl thermochemical process. The power plant's energy and exergy efficiencies are calculated as 56.71% and 53.59%, respectively.

There are numerous techniques to supplement freshwater from sea or ocean water. However, all these techniques require access to water resources, so their use is problematic, particularly in landlocked areas. In addition, these techniques need vast infrastructure for operation [4]. Atmospheric water harvesting (AWH) is a process that harvests air moisture. Moisture, as one of the sources of freshwater, exists all over the world. The volume of water in the atmosphere, which is estimated at 12,900 km^3, is six times the volume of all rivers in the world. This water source can provide part of the water needs in the agricultural, drinking, and even industrial sectors [22]. The United Nations, in its recent report, recognized AWH as a promising and low-cost alternative that can meet human consumption standards [23]. Furthermore, this process does not negatively affect the environment because the hydrological cycle naturally refills the harvested moisture [4].

Patel et al. [24] conducted an experimental study on an atmospheric water extracting (AWE) device. Their study was performed for different climates, and the results were reported. They showed that the AWE device performs best in hot and humid regions. Also, the obtained results showed that in the best condition, i.e., warm-humid condition, the freshwater production by this device is 1.78 l/h, and its power consumption is 0.75 kWh/l of water, while for mild and dry conditions, these values are respectively equal to 0.28 l/h and 4.71 kWh/l. Integration of atmospheric water harvesting units with renewable energy sources can increase the benefits of this process. Chaitanya et al. [23] have used Biomass gasification energy to power an off-grid refrigeration system that can harvest air humidity. The results of the thermodynamic analysis showed that if 1000 kg of Biomass is used, this system will be able to produce 800–1200 L of water. Also, they claimed that the produced water amount can meet 10–12% of drinking water needs in certain states of India. Energy and exergy analysis of a solar AWH has been performed by Salek et al. [25]. They investigated the system performance in different climates; accordingly, they studied three cities in Iran: Tehran, Bandar Abbas, and Ramsar. Their proposed system was able to produce approximately 400 L of water per month at its maximum production, while its specific energy consumption was equal to 3 kWh/l.

According to the literature review conducted on the research field, and also based on the results obtained from the authors' recent review paper [26] that reviewed the Biomass-based polygeneration systems, some of the existing gaps were recognized as follows:

- The implementation of municipal sewage sludge, as the feed of polygeneration systems, has received less attention. However, the improper disposal of wastewater in some areas has caused serious damage to the ecosystem and also has neglected a potential energy source.
- The use of sewage sludge to produce biogas through anaerobic digestion, and using the digested sludge to produce syngas through gasification, simultaneously in the same system, have not been investigated in previous studies. Also, the simultaneous conversion of sewage sludge into energy through both anaerobic digestion and gasification is limited.
- Powering atmospheric water harvesting units with renewable energy has recently become more popular, but researchers have focused more on using solar and wind energy. The integration of this unit as one of the subsystems of a power plant or a multigeneration system is a subject that has not been studied.
- Performed studies on renewable hydrogen production using syngas in multigeneration systems are limited. Obtained syngas from the gasification of various bio-wastes is a rich source of hydrogen. Utilizing this potential while controlling and recycling wastes and preventing their environmental hazards also uses this free resource.

In this way, the need to design a system to fill some gaps was felt. Accordingly, a new Biomass-based multigeneration system is designed to produce power, hydrogen, freshwater, and heating by receiving sewage sludge as bio-waste. The Brayton cycle in this system is fed with biogas obtained from the anaerobic digestion process of raw sludge. Also, digested sludge enters the gasifier to produce syngas. This system produces hydrogen in a gas–water shift reaction unit that feeds on syngas, and freshwater is obtained through the atmospheric water harvesting unit. In the design of this system, the maximum heat capacity of the produced gases has been used, and efforts have been made to integrate the subsystems so that the waste in the set is reduced as much as possible. In this way, while reducing the environmental effects of wastewater, its energy is recovered, and valuable products, including power, heating, freshwater, and hydrogen, are produced.

In this paper, in addition, to designing a system based on existing gaps with a new configuration, 4E (energy, exergy, exergoeconomic, and exergoenvironmental) analysis is implemented on it, and the impact of the system's key variables on the main performance criteria of the system is studied. In addition, a case study is considered for the Çiğli wastewater treatment plant located in Izmir-Turkey to reveal the benefits of this system. In this regard, the information about this treatment plant was prepared and the weather data, including the temperature and relative humidity of the environment, were also extracted.

2. System description

An overview of the whole system is shown in Fig. 1. The proposed system consists of a Biomass conversion subsystem (BCS), water–gas shift reaction unit (WGSRU), Brayton cycle (BC), atmospheric water harvesting unit (AWH), steam Rankine cycle (SRC) and organic Rankine cycles (ORC).

A more detailed description of the system and the activation sequence of its different parts can be described in six steps as follows:

First, the sewage sludge from the wastewater treatment plant enters the system as an input feed. This sludge is first anaerobically digested. During this process, Biomass is converted into biogas and digestate. Biogas contains about 60% (by volume) methane and 40% of carbon dioxide. This biogas is used as the fuel of the Brayton cycle. The incoming air from stream 7 passes through the preheater and enters the combustion chamber to react with biogas. Combustion gases enter the gas turbine to generate power. Then these gases are passed through the preheater to heat the incoming air. Next, these gases, which are still at a high temperature (544.9 °C), pass through the generator of the water-ammonia absorption refrigeration cycle to provide the heat required

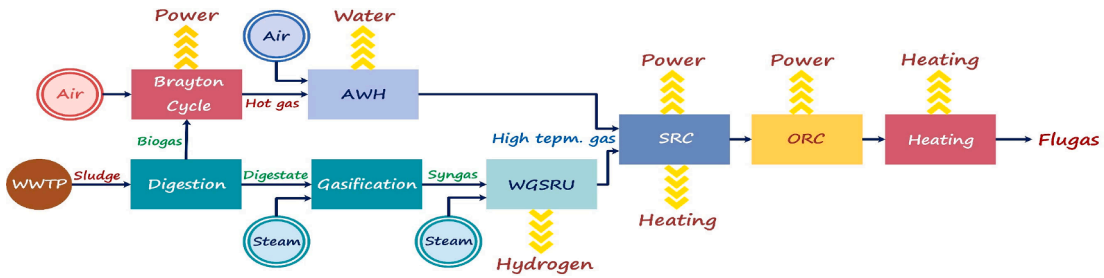

Fig. 1. An overview of the whole system.

for this cycle. The schematic of this step is shown in Fig. 2.

Second, a single-stage ammonia-water cycle, including absorber, pump, generator, rectifier, condenser, evaporator, expansion valves, and heat exchangers, has been used for harvesting atmospheric water. As shown in Fig. 3, which presents the schematic of this step, A low-pressure but strong solution of ammonia is pumped from the absorber to the generator, which operates at high pressure. The water and ammonia solution are separated in the generator; this separation happens through ammonia evaporation. Then the rectifier purifies the ammonia vapor. This vapor is condensed in the condenser, and after passing through the condenser-evaporator heat exchanger and throttling valve, it enters the evaporator. Liquid ammonia in the evaporator, which is very strong and has low pressure, is used to refrigerate the evaporator space. Next, ammonia evaporates and enters the absorber to repeat the cycle. In this way, the ammonia-water cycle is completed to produce cooling. In the following, the cooling produced by this cycle is used to harvest atmospheric water. This environmentally benign technology of freshwater production works based on the dew point temperature. The cooling power produced in the evaporator reduces the temperature of moist air to below its dew point, so liquid water is produced.

In the third step of integration, the digestate from the digestion process enters the gasifier to produce syngas in a steam gasification process. The produced syngas enters a Water-Gas Shift Reaction Unit and produces hydrogen during the reaction with water vapor. In this process, carbon monoxide reacts with water vapor and produces carbon dioxide and hydrogen. Hydrogen is removed as a valuable product of this unit, and the gas from the reaction enters the mixer to be mixed with the combustion gases that were previously used to provide the required heat for the absorption refrigeration cycle. This mixing increases the gas enthalpy (by enhancing the flow rate to 84.55 kg/s, and the temperature to 572 °C) for continuing the process and generating power. The schematic of this step is shown in Fig. 4.

As mentioned, stream 37 is a gas flow that is a mixture of gases from the water–gas shift reaction unit and from biogas combustion. In the fourth step, this gas is used to supply the heating power required for a steam Rankine cycle. The schematic of this step is illustrated in Fig. 5. In the steam Rankine cycle, steam travels through this cycle as a working fluid to generate power. Water is heated by hot gases in a heat exchanger and enters the steam turbine as superheated steam to generate power. Then, passing through the condenser, it liquefies and returns to the heat exchanger to repeat the cycle. Due to the high enthalpy difference in this equipment, it can be used to produce hot water. hot gases in stream 37, which was used to heat the Rankine cycle water, enter the following heat exchanger in stream 38 (at 348 °C) to provide the heating power required for the organic Rankine cycle.

Next, in the fifth step, Organic Rankine Cycles are used for power generation. This cycle supplies the required heating from stream 38. The schematic of this part of the system is presented in Fig. 6. Organic Rankine cycle 1 uses cyclohexane as the working fluid. This fluid is chemically stable and works efficiently when high-temperature heat sources are provided [27]. Cyclohexane passes through the mentioned heat exchanger to turn into superheated steam. Then it passes through the steam turbine and produces power during this process. Because cyclohexane is still a superheated vapor, its heat can evaporate isobutane in the second Rankine cycle evaporator. In the following, the remaining heat is removed through the condenser to become a saturated liquid and pumped into the heat exchanger again, and the cycle repeats in the same way. The same is true for the second Rankine cycle. However, the working fluid in the second cycle is isobutane. Also, unlike the other condensers in the system, the condenser of this cycle is cooled by air due to the low temperature of its associated streams [28]. As a common fluid in organic Rankine cycles, isobutane requires a lower temperature input for evaporation. Generally, this fluid performs well and is chemically stable and non-toxic [29].

The exhaust gas from the organic Rankine cycle heat exchanger still has a high enthalpy. This potential can be used to produce hot water. Finally, the flue gas leaves the system at 110 °C in the base case condition. The complete schematic of the system, which was completed after six stages of integration, is shown in Fig. 7.

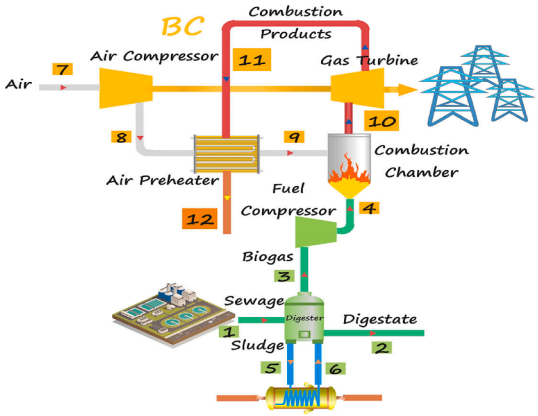

Fig. 2. Schematic diagram of the first part of the system.

3. Materials and methods

The analysis of this cycle has been done from the perspective of the first and second law of thermodynamics, and also the economic and environmental points of view. The mass and energy conservation equations, exergy balance equation, cost balance equation, and environmental impact equations are written and solved using engineering equation solver (EES) software.

For system modeling, the following general assumptions are considered [25,30–32]:

- The whole cycle is assumed to be in a steady state.
- The composition of air is 77.48% nitrogen, 20.59% oxygen, 1.90% water vapor, and 0.03% carbon dioxide.
- The temperature, pressure, and relative humidity of air are considered as 25 °C, 101.3 kPa, and 40%, respectively.
- All gases are considered ideal.

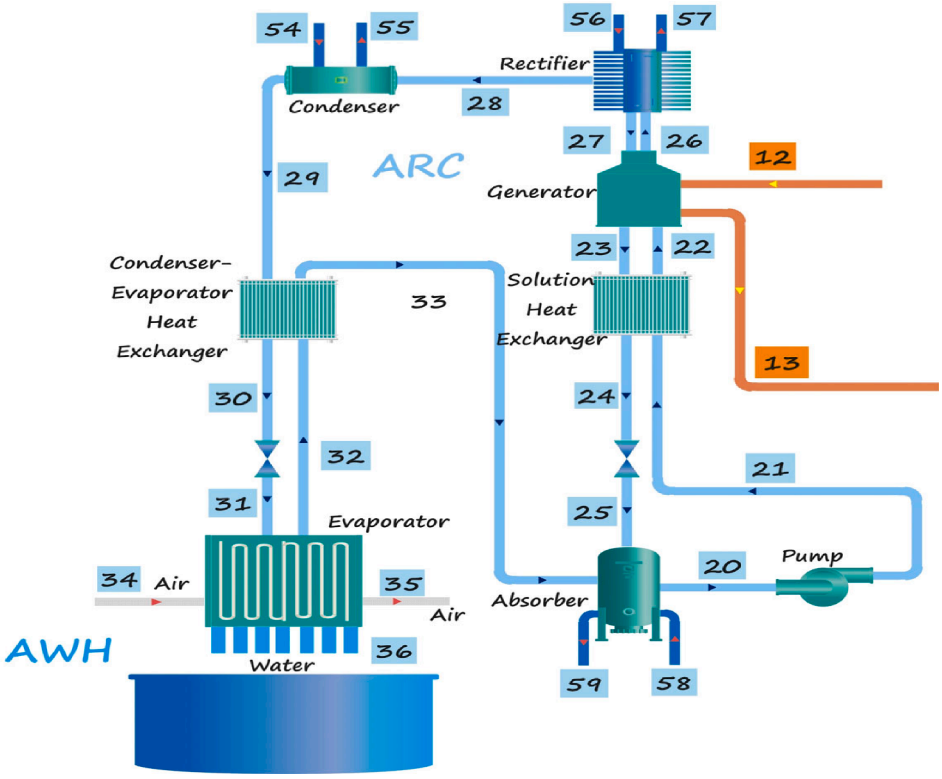

Fig. 3. Schematic diagram of the second step of the system integration.

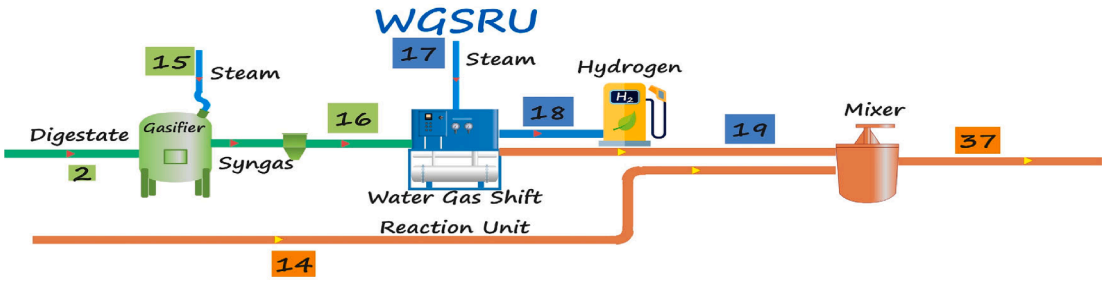

Fig. 4. Schematic diagram of the third step of the system integration.

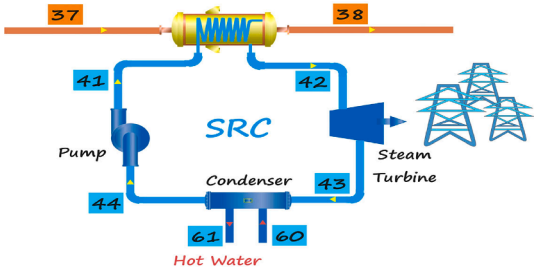

Fig. 5. Schematic diagram of the fourth step of the system integration.

- The pressure drops in pipes and heat exchangers are negligible. The pressure drop in the combustion chamber is 3%; the air preheater on the air side and gas side has 5% and 3% pressure drop, respectively.
- The heat loss in the equipment is ignored, while the heat loss in the combustion chamber is assumed to be 2% of the fuel's lower heating value (LHV).
- All turbines, compressors, and pumps operate in adiabatic mode. The isentropic efficiency of turbines and compressors is assumed to be 85%, and the isentropic efficiency of pumps is 90%.
- Potential and kinetic energy and exergy changes are negligible.
- In the economic analysis, the cost of all cooling water and air flows is assumed to be zero. Also, due to the different costs of steam in different production methods, it was assumed that the steam of both hydrogen production and gasification units are supplied from waste heat, and as a result, it is also considered equal to zero.

3.1. Energy and exergy analyses

The main equations of mass conservation, energy conservation, and exergy balance by implementing the mentioned assumptions, are expressed as follows [30]:

$$\sum_i \dot{m}_i = \sum_e \dot{m}_e \tag{1}$$

$$\sum_j \dot{Q}_j + \sum_i \dot{m}_i h_i = \dot{W} + \sum_e \dot{m}_e h_e \tag{2}$$

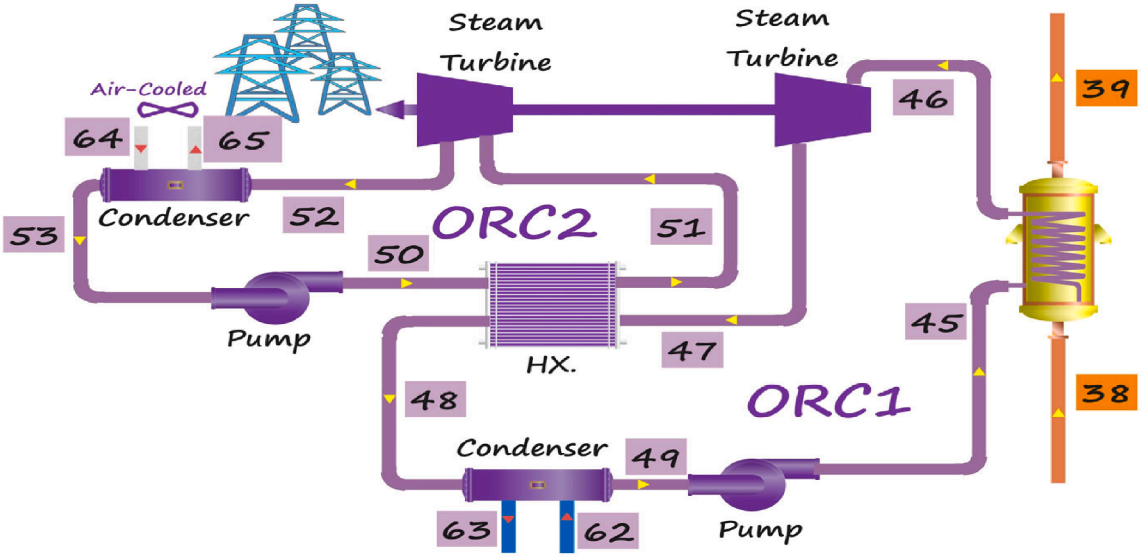

Fig. 6. Schematic diagram of the fifth step of the system integration.

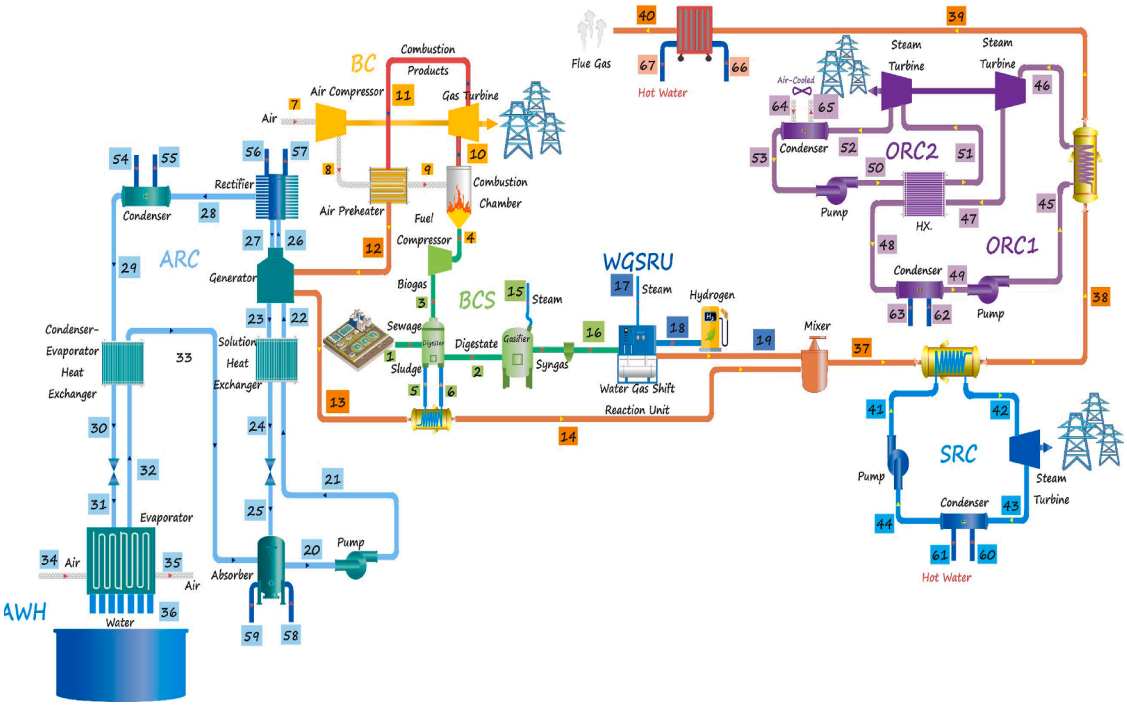

Fig. 7. Schematic diagram of the proposed system.

$$\sum_j \dot{Q}_j\left(1-\frac{T_0}{T_j}\right)+\sum_i \dot{m}_i ex_i = \dot{W}+\sum_e \dot{m}_e ex_e + \dot{E}x_D \tag{3}$$

The exergy of each stream is defined as the sum of its physical and chemical exergies. The following relations generally express these equations:

$$ex = ex^{ph} + ex^{ch} \tag{4}$$

$$ex^{ph} = h - h_0 - T_0(s - s_0) \tag{5}$$

$$ex^{ch} = \sum_k \frac{1}{y_k M_k}\left(\sum_k y_k \overline{ex}^{\circ} k + \overline{R}T_0 \sum_k y_k Ln(y_k)\right) \tag{6}$$

The mentioned equations are the basis of energy and exergy investigations of the system. In the following, the analysis performed on the subsystems and the equations related to each one has been discussed separately. The main equations necessary for the mathematical modeling of processes are explained, and the exergy equations for special cases are presented. Finally, the mass, energy, and exergy balance equations for each component are presented in Table 1.

- Anaerobic Digestion

The general reaction of the anaerobic digestion process that leads to the formation of methane and carbon dioxide is [33]:

$$C_nH_aO_b + \left(n-\frac{a}{4}-\frac{b}{2}\right)H_2O \rightarrow \left(\frac{n}{2}+\frac{a}{8}-\frac{b}{4}\right)CH_4 + \left(\frac{n}{2}-\frac{a}{8}+\frac{b}{4}\right)CO_2 \tag{7}$$

Table 1
The mass, energy, and exergy balance equations for components.

Cycle	Components	Balance equations
BCS	Digester	$\dot{m}_1 + \dot{m}_6 = \dot{m}_2 + \dot{m}_3 + \dot{m}_5$
		$\dot{m}_1 h_1 + \dot{m}_6 h_6 = \dot{m}_2 h_2 + \dot{m}_3 h_3 + \dot{m}_5 h_5$
		$\dot{E}x_{D,DIGBCS} = \dot{m}_1 ex_1 + \dot{m}_6 ex_6 - \dot{m}_2 ex_2 - \dot{m}_3 ex_3 - \dot{m}_5 ex_5$
	Heat Exchanger	$\dot{m}_6 = \dot{m}_5$
		$\dot{m}_5 h_5 + \dot{m}_{13} h_{13} = \dot{m}_6 h_6 + \dot{m}_{14} h_{14}$
		$\dot{E}x_{D,HXBCS} = \dot{m}_5 ex_5 + \dot{m}_{13} ex_{13} - \dot{m}_6 ex_6 - \dot{m}_{14} ex_{14}$
	Gasifier	$\dot{m}_2 + \dot{m}_{15} = \dot{m}_{16}$
		$\dot{Q}_{Gas} = a_1 \bar{h}^0_{H_2} + a_2 \bar{h}^0_{CO} + a_3 \bar{h}^0_{CO_2} + a_4 \bar{h}^0_{H_2O} + a_5 \bar{h}^0_{CH_4} - \bar{h}^0_{f,Biomass} - w\bar{h}^0_{H_2O(l)} - m\bar{h}^0_{H_2O}$
		$\dot{E}x_{D,GASBCS} = \dot{m}_2 ex_2 + \dot{m}_{15} ex_{15} - \dot{m}_{16} ex_{16} + \dot{Q}_{Gas}(1 - T_0/T_{Gasf})$
WGSRU	WGSRU	$\dot{m}_{16} + \dot{m}_{17} = \dot{m}_{18} + \dot{m}_{19}$
		$\dot{m}_{16} h_{16} + \dot{m}_{17} h_{17} = \dot{m}_{18} h_{18} + \dot{m}_{19} h_{19}$
		$\dot{E}x_{D,WGSRU} = \dot{m}_{16} ex_{16} + \dot{m}_{17} ex_{17} - \dot{m}_{18} ex_{18} - \dot{m}_{19} ex_{19}$
BC	Fuel	$\dot{m}_3 = \dot{m}_4$
	Compressor	$\dot{m}_3 h_3 + \dot{W}_{FC} = \dot{m}_4 h_4$
		$\dot{E}x_{D,FCBC} = \dot{m}_3 ex_3 + \dot{W}_{FC} - \dot{m}_4 ex_4$
	Air Compressor	$\dot{m}_7 = \dot{m}_8$
		$\dot{m}_7 h_7 + \dot{W}_{AC} = \dot{m}_8 h_8$
		$\dot{E}x_{D,ACBC} = \dot{m}_7 ex_7 + \dot{W}_{AC} - \dot{m}_8 ex_8$
	Air Preheater	$\dot{m}_8 + \dot{m}_{11} = \dot{m}_9 + \dot{m}_{12}$
		$\dot{m}_8 h_8 + \dot{m}_{11} h_{11} = \dot{m}_9 h_9 + \dot{m}_{12} h_{12}$
		$\dot{E}x_{D,APBC} = \dot{m}_8 ex_8 + \dot{m}_{11} ex_{11} - \dot{m}_9 ex_9 - \dot{m}_{12} ex_{12}$
	Combustion Chamber	$\dot{m}_4 + \dot{m}_9 = \dot{m}_{10}$
		$0 = -0.02\bar{\lambda}\overline{LHV} + \bar{h}_9 + \bar{\lambda}\bar{h}_4 - (1 + \bar{\lambda})\bar{h}_{10}$
		$\dot{E}x_{D,CCBC} = \dot{m}_4 ex_4 + \dot{m}_9 ex_9 - \dot{m}_{10} ex_{10}$
	Gas Turbine	$\dot{m}_{10} = \dot{m}_{11}$
		$\dot{m}_{10} h_{10} = \dot{m}_{11} h_{11} + \dot{W}_{GT}$
		$\dot{E}x_{D,GTBC} = \dot{m}_{10} ex_{10} - \dot{m}_{11} ex_{11} - \dot{W}_{GT}$
ARC & AWH	Absorber	$\dot{m}_{25} + \dot{m}_{33} + \dot{m}_{58} = \dot{m}_{20} + \dot{m}_{59}$
		$\dot{m}_{25} h_{25} + \dot{m}_{33} h_{33} + \dot{m}_{58} h_{58} = \dot{m}_{20} h_{20} + \dot{m}_{59} h_{59}$
		$\dot{E}x_{D,ABARC} = \dot{m}_{25} ex_{25} + \dot{m}_{33} ex_{33} + \dot{m}_{58} ex_{58} - \dot{m}_{20} ex_{20} - \dot{m}_{59} ex_{59}$
	Pump	$\dot{m}_{20} = \dot{m}_{21}$
		$\dot{m}_{20} h_{20} + \dot{W}_{pmp,ARC} = \dot{m}_{21} h_{21}$
		$\dot{E}x_{D,PMPARC} = \dot{m}_{20} ex_{20} + \dot{W}_{pmp,ARC} - \dot{m}_{21} ex_{21}$
	SHE	$\dot{m}_{21} + \dot{m}_{23} = \dot{m}_{22} + \dot{m}_{24}$
		$\dot{m}_{21} h_{21} + \dot{m}_{23} h_{23} = \dot{m}_{22} h_{22} + \dot{m}_{24} h_{24}$
		$\dot{E}x_{D,SHXARC} = \dot{m}_{21} ex_{21} + \dot{m}_{23} ex_{23} - \dot{m}_{22} ex_{22} - \dot{m}_{24} ex_{24}$
	Abs. Valve	$\dot{m}_{24} = \dot{m}_{25}$
		$\dot{m}_{24} h_{24} = \dot{m}_{25} h_{25}$
		$\dot{E}x_{D,VLVSARC} = \dot{m}_{24} ex_{24} - \dot{m}_{25} ex_{25}$
	Generator	$\dot{m}_{22} + \dot{m}_{27} + \dot{m}_{12} = \dot{m}_{23} + \dot{m}_{26} + \dot{m}_{13}$
		$\dot{m}_{22} h_{22} + \dot{m}_{27} h_{27} + \dot{m}_{12} h_{12} = \dot{m}_{23} h_{23} + \dot{m}_{26} h_{26} + \dot{m}_{13} h_{13}$
		$\dot{E}x_{D,GENARC} = \dot{m}_{22} ex_{22} + \dot{m}_{27} ex_{27} + \dot{m}_{12} ex_{12} - \dot{m}_{23} ex_{23} - \dot{m}_{26} ex_{26} - \dot{m}_{13} ex_{13}$
	Rectifier	$\dot{m}_{26} + \dot{m}_{56} = \dot{m}_{27} + \dot{m}_{28} + \dot{m}_{57}$
		$\dot{m}_{26} h_{26} + \dot{m}_{56} h_{56} = \dot{m}_{27} h_{27} + \dot{m}_{28} h_{28} + \dot{m}_{57} h_{57}$
		$\dot{E}x_{D,RECTARC} = \dot{m}_{26} ex_{26} + \dot{m}_{56} ex_{56} - \dot{m}_{27} ex_{27} - \dot{m}_{28} ex_{28} - \dot{m}_{57} ex_{57}$
	Condenser	$\dot{m}_{28} + \dot{m}_{54} = \dot{m}_{29} + \dot{m}_{55}$
		$\dot{m}_{28} h_{28} + \dot{m}_{54} h_{54} = \dot{m}_{29} h_{29} + \dot{m}_{55} h_{55}$
		$\dot{E}x_{D,CONDARC} = \dot{m}_{28} ex_{28} + \dot{m}_{54} ex_{54} - \dot{m}_{29} ex_{29} - \dot{m}_{55} ex_{55}$
	CEHE	$\dot{m}_{29} + \dot{m}_{32} = \dot{m}_{30} + \dot{m}_{33}$
		$\dot{m}_{29} h_{29} + \dot{m}_{32} h_{32} = \dot{m}_{30} h_{30} + \dot{m}_{33} h_{33}$
		$\dot{E}x_{D,CHXARC} = \dot{m}_{29} ex_{29} + \dot{m}_{32} ex_{32} - \dot{m}_{30} ex_{30} - \dot{m}_{33} ex_{33}$
	Evap. Valve	$\dot{m}_{30} = \dot{m}_{31}$
		$\dot{m}_{30} h_{30} = \dot{m}_{31} h_{31}$
		$\dot{E}x_{D,VLVCARC} = \dot{m}_{30} ex_{30} - \dot{m}_{31} ex_{31}$
	Evaporator	$\dot{m}_{31} + \dot{m}_{34} = \dot{m}_{32} + \dot{m}_{35} + \dot{m}_{36}$
		$\dot{m}_{31} h_{31} + \dot{m}_{34} h_{34} = \dot{m}_{32} h_{32} + \dot{m}_{35} h_{35} + \dot{m}_{36} h_{36}$
		$\dot{E}x_{D,EVAPARC} = \dot{m}_{31} ex_{31} + \dot{m}_{34} ex_{34} - \dot{m}_{32} ex_{32} - \dot{m}_{35} ex_{35} - \dot{m}_{36} ex_{36}$
Mixer	Mixer	$\dot{m}_{14} + \dot{m}_{19} = \dot{m}_{37}$
		$\dot{m}_{14} h_{14} + \dot{m}_{19} h_{19} = \dot{m}_{37} h_{37}$
		$\dot{E}x_{D,MIXER} = \dot{m}_{14} ex_{14} + \dot{m}_{19} ex_{19} - \dot{m}_{37} ex_{37}$
SRC	Heat Exchanger	$\dot{m}_{37} + \dot{m}_{41} = \dot{m}_{38} + \dot{m}_{42}$
		$\dot{m}_{37} h_{37} + \dot{m}_{41} h_{41} = \dot{m}_{38} h_{38} + \dot{m}_{42} h_{42}$
		$\dot{E}x_{D,HXSRC} = \dot{m}_{37} ex_{37} + \dot{m}_{41} ex_{41} - \dot{m}_{38} ex_{38} - \dot{m}_{42} ex_{42}$
	Pump	$\dot{m}_{44} = \dot{m}_{41}$
		$\dot{m}_{44} h_{44} + \dot{W}_{pmp,SRC} = \dot{m}_{41} h_{41}$
		$\dot{E}x_{D,PUSRC} = \dot{m}_{44} ex_{44} + \dot{W}_{pmp,SRC} - \dot{m}_{41} ex_{41}$
	Turbine	$\dot{m}_{42} = \dot{m}_{43}$
		$\dot{m}_{42} h_{42} = \dot{m}_{43} h_{43} + \dot{W}_{ST,SRC}$
		$\dot{E}x_{D,TUSRC} = \dot{m}_{42} ex_{42} - \dot{m}_{43} ex_{43} - \dot{W}_{ST,SRC}$
	Condenser	$\dot{m}_{43} + \dot{m}_{60} = \dot{m}_{44} + \dot{m}_{61}$
		$\dot{m}_{43} h_{43} + \dot{m}_{60} h_{60} = \dot{m}_{44} h_{44} + \dot{m}_{61} h_{61}$
		$\dot{E}x_{D,CDSRC} = \dot{m}_{43} ex_{43} + \dot{m}_{60} ex_{60} - \dot{m}_{44} ex_{44} - \dot{m}_{61} ex_{61}$
ORC	Heat Exchanger 1	$\dot{m}_{38} + \dot{m}_{45} = \dot{m}_{39} + \dot{m}_{46}$
		$\dot{m}_{38} h_{38} + \dot{m}_{45} h_{45} = \dot{m}_{39} h_{39} + \dot{m}_{46} h_{46}$
		$\dot{E}x_{D,HXORC1} = \dot{m}_{38} ex_{38} + \dot{m}_{45} ex_{45} - \dot{m}_{39} ex_{39} - \dot{m}_{46} ex_{46}$
	Pump 1	$\dot{m}_{49} = \dot{m}_{45}$
		$\dot{m}_{49} h_{49} + \dot{W}_{pmp,ORC1} = \dot{m}_{45} h_{45}$
		$\dot{E}x_{D,PUORC1} = \dot{m}_{49} ex_{49} + \dot{W}_{pmp,ORC1} - \dot{m}_{45} ex_{45}$
	Pump 2	$\dot{m}_{53} = \dot{m}_{50}$
		$\dot{m}_{53} h_{53} + \dot{W}_{pmp,ORC2} = \dot{m}_{50} h_{50}$
		$\dot{E}x_{D,PUORC2} = \dot{m}_{53} ex_{53} + \dot{W}_{pmp,ORC2} - \dot{m}_{50} ex_{50}$
	Turbine 1	$\dot{m}_{46} = \dot{m}_{47}$
		$\dot{m}_{46} h_{46} = \dot{m}_{47} h_{47} + \dot{W}_{ST,ORC1}$
		$\dot{E}x_{D,TUORC1} = \dot{m}_{46} ex_{46} - \dot{m}_{47} ex_{47} - \dot{W}_{ST,ORC1}$
	Turbine 2	$\dot{m}_{51} = \dot{m}_{52}$
		$\dot{m}_{51} h_{51} = \dot{m}_{52} h_{52} + \dot{W}_{ST,ORC2}$
		$\dot{E}x_{D,TUORC2} = \dot{m}_{51} ex_{51} - \dot{m}_{52} ex_{52} - \dot{W}_{ST,ORC2}$
	Condenser 1	$\dot{m}_{48} + \dot{m}_{62} = \dot{m}_{49} + \dot{m}_{63}$
		$\dot{m}_{48} h_{48} + \dot{m}_{62} h_{62} = \dot{m}_{49} h_{49} + \dot{m}_{63} h_{63}$
		$\dot{E}x_{D,CDORC1} = \dot{m}_{48} ex_{48} + \dot{m}_{62} ex_{62} - \dot{m}_{49} ex_{49} - \dot{m}_{63} ex_{63}$
	Condenser 2	$\dot{m}_{52} + \dot{m}_{64} = \dot{m}_{53} + \dot{m}_{65}$
		$\dot{m}_{52} h_{52} + \dot{m}_{64} h_{64} + \dot{W}_{Fan} = \dot{m}_{53} h_{53} + \dot{m}_{65} h_{65}$
		$\dot{E}x_{D,ACCORC2} = \dot{m}_{52} ex_{52} + \dot{m}_{64} ex_{64} + \dot{W}_{Fan} - \dot{m}_{53} ex_{53} - \dot{m}_{65} ex_{65}$
	Heat Exchanger 2	$\dot{m}_{47} + \dot{m}_{50} = \dot{m}_{48} + \dot{m}_{51}$
		$\dot{m}_{47} h_{47} + \dot{m}_{50} h_{50} = \dot{m}_{48} h_{48} + \dot{m}_{51} h_{51}$
		$\dot{E}x_{D,HXORC1} = \dot{m}_{47} ex_{47} + \dot{m}_{50} ex_{50} - \dot{m}_{48} ex_{48} - \dot{m}_{51} ex_{51}$
Heater	Heater	$\dot{m}_{39} + \dot{m}_{66} = \dot{m}_{40} + \dot{m}_{67}$
		$\dot{m}_{39} h_{39} + \dot{m}_{66} h_{66} = \dot{m}_{40} h_{40} + \dot{m}_{67} h_{67}$
		$\dot{E}x_{D,HEATER} = \dot{m}_{39} ex_{39} + \dot{m}_{66} ex_{66} - \dot{m}_{40} ex_{40} - \dot{m}_{67} ex_{67}$

This process takes place in a digester whose temperature is kept constant at 35 °C. Considering that a well-designed digester destroys at least 70% of volatile solids, the biogas obtained from the reaction will contain about 60% of methane (by volume) and 40% of carbon dioxide [34,35].

To calculate the required heat of the process, considering that a large part of the Biomass is moisture, the amount of heat needed to change the water temperature from the ambient temperature to the digestion temperature will be equivalent to the heat required for the digestion process [34]:

$$\dot{Q}_{Dig} = \dot{m}_{MC} C_{p,water} (T_{Dig} - T_0) \tag{8}$$

The physical and chemical exergy of the raw and digested Biomass can be calculated using the exergy relations of organic matter [36]:

$$ex^{ph}_{OM} = C_p \left(T - T_0 - T_0 \ln\left(\frac{T}{T_0}\right) \right) \tag{9}$$

$$ex^{ch}_{OM} = 363.439C + 1075.633H - 86.308O + 4.14N + 190.798S - 21.1A \ [kJ/kg] \tag{10}$$

- Brayton Cycle

The Brayton cycle consists of a fuel compressor, an air compressor, an air preheater, a combustion chamber, and a gas turbine. The properties related to the output flows of the fuel and air compressors and gas turbine are calculated using the isentropic efficiency relations given as follows [37]:

$$\eta_{s,FC} = \frac{\overline{h}_{4s} - \overline{h}_3}{\overline{h}_4 - \overline{h}_3} \tag{11}$$

$$\eta_{s,AC} = \frac{\overline{h}_{8s} - \overline{h}_7}{\overline{h}_8 - \overline{h}_7} \tag{12}$$

$$\eta_{s,GT} = \frac{\overline{h}_{11s} - \overline{h}_{10}}{\overline{h}_{11} - \overline{h}_{10}} \tag{13}$$

The combustion chamber of this cycle is fed by biogas. The amount of air entering the cycle is determined by the fuel–air ratio. This ratio on a molar basis is defined as [38]:

$$\overline{\lambda} = \frac{\dot{n}_F}{\dot{n}_a} \tag{14}$$

The combustion reaction equation for the complete combustion of biogas is written as follows:

$$\overline{\lambda}[x_{CH_4}CH_4 + x_{CO_2}CO_2] + [0.7748N_2 + 0.2059O_2 + 0.0003CO_2 + 0.019H_2O] \rightarrow [1+\overline{\lambda}][Y_{N_2}N_2 + Y_{O_2}O_2 + Y_{CO_2}CO_2 + Y_{H_2O}H_2O] \tag{15}$$

With the balance of carbon, hydrogen, oxygen, and nitrogen, the mole fraction of the components of the combustion products are:

$$Y_{N_2} = \frac{0.7748}{1+\overline{\lambda}} \tag{16}$$

$$Y_{O_2} = \frac{0.2059 - 2x_{CH_4}}{1+\overline{\lambda}} \tag{17}$$

$$Y_{CO_2} = \frac{0.0003 + \overline{\lambda}}{1+\overline{\lambda}} \tag{18}$$

$$Y_{H_2O} = \frac{0.019 + 2x_{CH_4}}{1+\overline{\lambda}} \tag{19}$$

As it was mentioned in the assumptions, the heat loss of the combustion chamber is assumed to be 2% of the LHV of the fuel. So, the energy balance for the combustion chamber is written as follows:

$$0 = -0.02\overline{\lambda}\overline{LHV} + \overline{h}_9 + \overline{\lambda}\overline{h}_4 - (1+\overline{\lambda})\overline{h}_{10} \tag{20}$$

By inserting appropriate expressions for each term, the fuel–air ratio can be obtained through the following equation:

$$\overline{\lambda} = \frac{0.7748\Delta\overline{h}_{N_2} + 0.2059\Delta\overline{h}_{O_2} + 0.0003\Delta\overline{h}_{CO_2} + 0.019\Delta\overline{h}_{H_2O}}{\overline{h}_4 - 0.02\overline{LHV} - (-2x_{CH_4}\overline{h}_{O_2} + \overline{h}_{CO_2} + 2x_{CH_4}\overline{h}_{H_2O})_{(T_{10})}} \tag{21}$$

The lower heating value of the biogas at 25 °C and 101.3 kPa can be calculated as [37]:

$$\overline{LHV} = \overline{H}_{prod} - \overline{H}_{react} = \sum N_p\overline{h}^0_{f,p} - \sum N_r\overline{h}^0_{f,r} \tag{22}$$

- Steam Gasification

The global reaction of the steam gasification process is as follows [39]:

$$CH_aO_b + wH_2O + mH_2O \rightarrow a_1H_2 + a_2CO + a_3CO_2 + a_4H_2O + a_5CH_4 \tag{23}$$

CH_aO_b is the chemical formula of Biomass that is simplified. Given that in an extensive range of Biomass feedstocks, sulfur and nitrogen levels are insignificant, the equation below is valid [40]:

$$a = 1.4125b + 0.5004 \tag{24}$$

Also, the required relations for a and b calculation are as [41]:

$$a = \frac{M_C \times H}{M_H \times C} \tag{25}$$

$$b = \frac{M_C \times O}{M_O \times C} \tag{26}$$

In the global reaction of steam gasification, m is the mole of steam added per mole of dry ash-free Biomass, and w is the moisture per mole of dry ash-free Biomass. These parameters can be determined as follows [42]:

$$STBM = \frac{M_{H_2O} \times m}{M_{Biomass} + M_{H_2O} \times w} \tag{27}$$

$$w = \frac{M_{Biomass} \times MC}{M_{H_2O} \times (1 - MC)} \tag{28}$$

To calculate the coefficients of a_1 to a_5, molar balance is used for the components, but more than these equations are needed, and the equilibrium constants relationships should also be used.

$$\text{Carbon balance}: a_1 + a_3 + a_5 = 1 \tag{29}$$

$$\text{Hydrogen balance}: a + 2w + 2m = 2a_1 + 2a_4 + 4a_5 \tag{30}$$

$$\text{Oxygen balance}: b + w + m = a_2 + 2a_3 + a_4 \tag{31}$$

The following equilibrium reactions are the main reactions that take place in the reduction zone of the gasifier [39]:

$$\text{Boudouard reaction}: C + CO_2 \rightarrow 2CO \tag{32}$$

$$\text{Water} - \text{gas reaction}: C + H_2O \rightarrow CO + H_2 \tag{33}$$

$$\text{Water} - \text{gas shift reaction}: CO + H_2O \rightarrow CO_2 + H_2 \tag{34}$$

$$\text{Methane reaction}: C + 2H_2 \rightarrow CH_4 \tag{35}$$

Equilibrium constants for water–gas shift and methane reactions are given as [43]:

$$K_1 = \frac{P_{CO_2}P_{H_2}}{P_{CO}P_{H_2O}} = \frac{a_3a_1}{a_2a_4} \tag{36}$$

$$K_2 = \frac{P_{CH_4}}{P_{H_2}{}^2} = \frac{a_5(a_1 + a_2 + a_3 + a_4 + a_5)}{a_1{}^2} \tag{37}$$

The equilibrium constant is a function of temperature and is expressed in terms of Gibbs free energy:

$$LnK = \frac{-\Delta\overline{g}}{\overline{R}T_g} \tag{38}$$

where $\overline{R}$ is the universal gas constant 8.314 $kJ/kmol$. K and $\Delta\overline{g}$ can be determined as follows:

$$\Delta\overline{g} = \Delta\overline{h} - T_g\Delta\overline{s} \tag{39}$$

Therefore, for water–gas shift and methane reactions, respectively:

$$\Delta\overline{g}_1 = (\overline{h}^0_{CO_2} + \overline{h}^0_{H_2} - \overline{h}^0_{CO} - \overline{h}^0_{H_2O}) - T_g(\overline{s}^0_{CO_2} + \overline{s}^0_{H_2} - \overline{s}^0_{CO} - \overline{s}^0_{H_2O}) \tag{40}$$

$$\Delta\overline{g}_2 = (\overline{h}^0_{CH_4} - 2\overline{h}^0_{H_2} - \overline{h}^0_{C}) - T_g(\overline{s}^0_{CH_4} - 2\overline{s}^0_{H_2} - \overline{s}^0_{C}) \tag{41}$$

Steam to Biomass ratio is considered a known parameter in modeling. Gasification of Biomass using other agents is autothermal, but gasification using CO_2 and steam agents is allothermal because the steam gasification is a highly endothermic reaction, so the heat of this process ($\dot{Q}_{Gas}$) is provided by an external heat source [41] and calculated as follows [43]:

$$\dot{Q}_{Gas} = a_1\overline{h}^0_{H_2} + a_2\overline{h}^0_{CO} + a_3\overline{h}^0_{CO_2} + a_4\overline{h}^0_{H_2O} + a_5\overline{h}^0_{CH_4} - \overline{h}^0_{f,Biomass} - w\overline{h}^0_{H_{2O(l)}} \tag{42}$$

The following equation is used to calculate the LHV of syngas [17]:

$$LHV_{syngas} = \sum_i n_i \times \overline{LHV}_i \tag{43}$$

where n_i and $\overline{LHV}_i$ represent the mole flow rate and molar LHV of the gas components.

- Water-Gas Shift Reaction

A water–gas shift reaction unit was applied to convert the syngas to hydrogen. This unit is considered adiabatic. The general reaction of the water gas shift process is as follows [18]:

$$CO + H_2O \rightarrow CO_2 + H_2 \tag{44}$$

As it is known from the reaction equation, carbon monoxide in the syngas reacts with water vapor and produces carbon dioxide and hydrogen. Hydrogen is a valuable fuel that, if produced from syngas, goes through an environmentally benign life cycle [16].

- Rankine Cycles

The Rankine cycles in this system work through the energy recovery of the flue gas, which is a mixture of combustion product gases and exhaust gas from the WGSRU. The temperature of the mixed flow can be calculated using its enthalpy. The enthalpy of mixed gas (state 37) is determined using the following equation [44]:

$$h_{37} = \frac{\dot{m}_{14}}{\dot{m}_{14} + \dot{m}_{19}}h_{14} + \frac{\dot{m}_{19}}{\dot{m}_{14} + \dot{m}_{19}}h_{19} \tag{45}$$

The properties related to the outlet streams of all turbines and pumps in the steam/organic Rankine cycles are determined using the isentropic efficiencies that define as below:

$$\eta_{s,ST} = \frac{\overline{h}_{e,s} - \overline{h}_i}{\overline{h}_e - \overline{h}_i} \tag{46}$$

$$\eta_{s,P} = \frac{\overline{h}_i - \overline{h}_{e,s}}{\overline{h}_i - \overline{h}_e} \tag{47}$$

The condenser of the second organic Rankine cycle is cooled by air due to the low temperature of the associated streams. It is assumed that the power consumed by the air-cooled condenser fans is 0.15 kW per kg/s of air flow [45]:

$$\dot{W}_{Fan} = 0.15\dot{m}_{64} \tag{48}$$

- Atmospheric Water Harvesting

The AWH cycle analysis has been performed by applying the first law of thermodynamics. Dry air mass flow rate is defined as [46]:

$$\dot{m}_{34} = \dot{m}_{34DA}(1 + \omega_{34}) \tag{49}$$

$$\dot{m}_{35} = \dot{m}_{35DA}(1 + \omega_{35}) \tag{50}$$

$$\dot{m}_{DA} = \dot{m}_{34DA} = \dot{m}_{35DA} \tag{51}$$

Hence, produced water mass flow rate is determined as:

$$\dot{m}_{water} = \dot{m}_{DA}\omega_{34} - \dot{m}_{DA}\omega_{35} \tag{52}$$

where ω is the humidity ratio of air which can be obtained by psychrometric charts. This paper uses the EES software library, which has thermodynamic properties of humid air. The value of the humidity ratio is obtained by having three variables: temperature, pressure, and relative humidity.

Also, for the evaporator, the following relationship is established:

$$\dot{Q}_{evaporator} = \dot{m}_{DA}(h_{34} - h_{35}) - \dot{m}_{36}h_{36} \tag{53}$$

Total power consumption per kg of water generation in one hour expressed as:

$$WP = \frac{\dot{W}_{pmp,SRC} + \dot{Q}_{gen}}{\dot{m}_{36} \times 3600} \tag{54}$$

The chemical exergy of the refrigerant cycle working fluid and the physical exergy of humid air are calculated from special relationships. Specific chemical exergy for the mixture "refrigerant-absorbent" can be determined as [47]:

$$ex^{ch} = x \bullet ex^{ch}_{\text{refrigerant}} + (1 - x) \bullet ex^{ch}_{\text{absorbent}} \tag{55}$$

where $ex^{ch}_{\text{refrigerant}} = ex^{ch}_{NH_3} = 337900kJ/kmol$, and $ex^{ch}_{\text{absorbent}} = ex^{ch}_{H_2O} = 900kJ/kmol$ were used.

The physical exergy of humid air is defined as below [48]:

$$ex_{ha} = (c_{p,a} + \omega c_{p,w}) \bullet T_0\left(\frac{T}{T_0} - 1 - \ln\left(\frac{T}{T_0}\right)\right) + (1 + \widetilde{\omega})R_aT_0ln\left(\frac{P}{P_0}\right) + R_aT_0\left[\ln\left(\frac{1 + \widetilde{\omega}_0}{1 + \widetilde{\omega}}\right) + \widetilde{\omega}\ln\left(\frac{\widetilde{\omega}(1 + \widetilde{\omega}_0)}{\widetilde{\omega}_0(1 + \widetilde{\omega})}\right)\right] \tag{56}$$

where $\widetilde{\omega}$ is the vapor mole fraction ratio which $\widetilde{\omega} = 1.608\omega$, R_a is the gas constant of air that is equal to 0.287 kJ/kg.K, and subscript 0 refers to the reference state.

- Performance criteria

The evaluation of this system is based on energy and exergy analysis. The total exergy destruction rate of the whole system and exergy destruction ratio can be calculated from the following relations, respectively:

$$\dot{E}x_{D,Tot} = \sum_k \dot{E}x_{D,k} \tag{57}$$

$$Y_{D,k} = \frac{\dot{E}x_{D,k}}{\dot{E}x_{D,Tot}} \tag{58}$$

The exergetic performance coefficient is defined as the ratio of the total power generation rate to the total exergy destruction rate. This factor includes both energy and exergy factors and can be beneficial for engineering decisions [49]:

$$EPC = \frac{\dot{W}_{net}}{\dot{E}x_{D,Tot}} \tag{59}$$

where:

$$\dot{W}_{net} = \dot{W}_{GT} + \dot{W}_{ST,SRC} + \dot{W}_{ST,ORC1} + \dot{W}_{ST,ORC2} - (\dot{W}_{AC} + \dot{W}_{FC} + \dot{W}_{pmp,SRC} + \dot{W}_{pmp,ORC1} + \dot{W}_{pmp,ORC2} + \dot{W}_{pmp,ARC} + \dot{W}_{Fan}) \tag{60}$$

The main performance criteria for the thermodynamic evaluation of the system are energy and exergy efficiencies. Efficiency is usually defined as the ratio of useful output to the total input. In Table 2, each subsystem's energy and exergy efficiencies are provided separately.

To evaluate the overall system performance, the overall energy and exergy efficiencies have been considered:

$$\eta_{en} = \frac{\dot{W}_{net} + \dot{Q}_{Heating} + \dot{m}_{H_2} LHV_{H_2} + \dot{m}_{water} h_{water}}{\dot{m}_{Biomass} LHV_{Biomass} + \dot{Q}_{Gas} + \dot{m}_{15} h_{15} + \dot{m}_{17} h_{17}} \tag{61}$$

$$\psi_{ex} = \frac{\dot{W}_{net} + (\dot{m}_{61}(ex_{61} - ex_{60}) + \dot{m}_{67}(ex_{67} - ex_{66})) + \dot{m}_{H_2} ex_{H_2} + \dot{m}_{water} ex_{water}}{\dot{m}_{Biomass} ex_{Biomass} + \dot{Q}_{Gas}\left(1 - T_0/T_{Gasf}\right) + \dot{m}_{15} ex_{15} + \dot{m}_{17} ex_{17}} \tag{62}$$

where:

$$\dot{Q}_{Heating} = \dot{Q}_{Heater} + \dot{Q}_{Cond,SRC} = \dot{m}_{61}(h_{61} - h_{60}) + \dot{m}_{67}(h_{67} - h_{66}) \tag{63}$$

3.2. Exergoeconomic analysis

Exergoeconomic analysis combines exergy investigations with economic principles to study the system from exergy and economics perspectives. This analysis covers the inadequacy of energy and exergy analyses by providing economic results for decision-makers. The cost balance equation as the base of this evaluation is expressed as [30]:

$$\sum_{in} \dot{C}_{in,k} + \dot{C}_{q,k} + \dot{Z}_k = \sum_{out} \dot{C}_{out,k} + \dot{C}_{w,k} \tag{64}$$

where $\dot{C}$ refers to the cost rate and $\dot{Z}_k$ is the capital investment cost of components. The cost rate is obtained as [30]:

$$\dot{C} = c \times \dot{E}x \tag{65}$$

where c is the specified cost per unit of exergy.

Capital investment cost of components that consists of operation and maintenance costs is defined as [50]:

$$\dot{Z}_k = \frac{Z_k \bullet CRF \bullet \phi}{N \times 3600} \tag{66}$$

Here N and ϕ are the annual duration of operation hours and maintenance factor, respectively. Additionally, CRF is the capital recovery factor that is given by [50]:

$$CRF = \frac{i(1+i)^n}{(1+i)^n - 1} \tag{67}$$

where i and n represent the interest rate and lifetime of the project, respectively. The values of the mentioned parameters are presented in Table 3.

The cost of k_{th} component (Z_k) are listed in Table 4. The cost of the water–gas shift reactor is estimated through the six-tenth rule [51]. The values obtained from the cost equations should be updated to the current year, utilizing Chemical Engineering Plant Cost Index (CEPCI) [52]:

Table 2
The energy and exergy efficiencies of subsystems.

cycle	Energy Efficiency	Exergy Efficiency
ARC	$COP_{en} = \frac{\dot{Q}_{evap}}{\dot{Q}_{gen} + \dot{W}_{pmp,ARC}}$	$COP_{ex} = \frac{\dot{E}x^{Q}_{evap}}{\dot{W}_P + \dot{E}x^{Q}_{gen}}$
BC	$\eta = \frac{\dot{W}_{GT} - \dot{W}_{AC} - \dot{W}_{FC}}{\dot{m}_4 LHV_4}$	$\psi = \frac{\dot{W}_{GT} - \dot{W}_{AC} - \dot{W}_{FC}}{\dot{m}_4 ex_4}$
WGSRU	$\eta = \frac{\dot{m}_{18} LHV_{H_2}}{\dot{m}_{16} h_{16} - \dot{m}_{19} h_{19} + \dot{m}_{17} h_{17}}$	$\psi = \frac{\dot{m}_{18} ex_{18}}{\dot{m}_{16} ex_{16} - \dot{m}_{19} ex_{19} + \dot{m}_{17} ex_{17}}$
SRC	$\eta = \frac{\dot{W}_{ST,SRC} - \dot{W}_{pmp,SRC}}{\dot{m}_{37} h_{37} - \dot{m}_{38} h_{38}}$	$\psi = \frac{\dot{W}_{ST,SRC} - \dot{W}_{pmp,SRC}}{\dot{m}_{37} ex_{37} - \dot{m}_{38} ex_{38}}$
ORC	$\eta = \frac{\dot{W}_{ST,ORC1} + \dot{W}_{ST,ORC2} - (\dot{W}_{pmp,ORC1} + \dot{W}_{pmp,ORC2} + \dot{W}_{Fan})}{\dot{m}_{38} h_{38} - \dot{m}_{39} h_{39}} \psi = \frac{\dot{W}_{ST,ORC1} + \dot{W}_{ST,ORC2} - (\dot{W}_{pmp,ORC1} + \dot{W}_{pmp,ORC2} + \dot{W}_{Fan})}{\dot{m}_{38} ex_{38} - \dot{m}_{39} ex_{39}}$	

$$Z_p = Z_0\left(\frac{\text{CEPCI}_p}{\text{CEPCI}_0}\right) \tag{68}$$

Here p and 0 subscripts refer to the present and the original year. The latest available CEPCI was 808.9 (December 2022), used as the present year index [53].

Total cost rate of this system is considered as the sum of the fuel cost rate, the rate of the penalty cost of greenhouse gas emission, the heat cost rate for the gasifier, the cost rate of exergy destruction, and the total capital investment cost of the components [54,55]:

$$\dot{C}_{TOTAL} = \dot{C}_f + \dot{C}_{env} + \dot{C}_Q + \dot{C}_{D,TOTAL} + \sum_k \dot{Z}_k \tag{69}$$

Each of the above parameters is defined as follows:

$$\dot{C}_f = c_f \bullet \dot{E}x_f \tag{70}$$

$$\dot{C}_{env} = c_{CO_2} \bullet \dot{m}_{CO_2,40} \tag{71}$$

$$\dot{C}_Q = c_q \bullet \dot{Q}_{Gas} \tag{72}$$

$$\dot{C}_{D,TOTAL} = \sum_k \dot{C}_{D,k} \quad ; \quad \dot{C}_{D,k} = c_{F,k} \bullet \dot{E}x_{D,k} \tag{73}$$

where c_f is cost of Biomass per unit of exergy (2 $/GJ) [56], c_{CO_2} is the unit damage cost of CO_2 (0.024 $/kg) [57], c_q is the specific cost of heating energy (0.04 $/kWh) [58], and $c_{F,k}$ is the unit cost of fuel of the kth component.

The unit cost of each product of the system and the unit cost of total products of the multigeneration system are expressed respectively as [59]:

$$c_{product} = \frac{\dot{C}_{product}}{\dot{E}x_{product}} \tag{74}$$

$$c_{p,TOTAL} = \frac{\dot{C}_{W,NET} + \dot{C}_{61} + \dot{C}_{67} + \dot{C}_{18} + \dot{C}_{36}}{\dot{W}_{net} + \dot{E}x_{61} + \dot{E}x_{p67} + \dot{E}x_{18} + \dot{E}x_{36}} \tag{75}$$

In addition, since the cost sources of a component are classified into two categories of non-exergy-related costs and the costs related to exergy destruction, the exergoeconomic factor is defined to evaluate the performance of each component [59]:

Table 3
Cost indices.

Parameters	Values	Units
Annual duration of operation hours (N)	8000	Hours
Maintenance factor (ϕ)	1.06	–
Interest rate (i)	0.10	–
Lifetime of the project (n)	20	Years

$$f_k = \frac{\dot{Z}_k}{\dot{Z}_k + \dot{C}_{D,k}} \tag{76}$$

3.3. Exergoenvironmental analysis

Exergoenvironmental analysis combines exergy and environmental analysis to simultaneously study the system from exergy and environmental points of view. The exergoenvironment factor, which is defined as follows, shows the harmful effects of irreversibility on the environment [60,66]:

$$f_{ei} = \frac{\dot{E}x_{D,Tot}}{\dot{E}x_{in}} \tag{77}$$

If this factor is significant, the ratio of exergy destruction rate to input exergy rate and consequently the negative effects on the environment is high.

The next important factor in exergoenvironmental analysis is the environmental damage effectiveness factor, which is calculated as follows [60,66]:

$$\theta_{ei} = f_{ei} \bullet C_{ei} \tag{78}$$

Table 4
Cost functions of system components.

Components	Z_k[$]	Ref.
Compressor	$Z = \frac{c'_1 \dot{m}}{c'_2 - \eta_{SC}} \left(\frac{P_{out}}{P_{in}}\right) ln\left(\frac{P_{out}}{P_{in}}\right) c'_1 = 44.71\$/(kg/s)$, $c'_2 = 0.95$	[60]
Gas turbine	$Z = \frac{c'_3 \dot{m}}{c'_4 - \eta_{ST}} \ln\left(\frac{P_{in}}{P_{out}}\right) \left(1 + e^{c'_5 (T_{in} - 1570)}\right) c'_3 = 301.45\$/(kg/s), c'_4 = 0.94, c'_5 = 0.025K^{-1}$	[60]
Combustion chamber	$Z = \frac{c'_6 \dot{m}}{c'_7 - \frac{P_{out}}{P_{in}}} (1 + e^{c'_8 (T_{out} - 1540)}) c'_6 = 28.98\$/(kg/s)$, $c'_7 = 0.995, c'_8 = 0.015K^{-1}$	[60]
Heat exchangers	$Z = c'_9 (A_{HE}/0.093)^{0.78} c'_9 = 130\$/(m^2)^{0.78}$	[31]
Digester	$Z = 350000 (\frac{VT}{21000})^{0.75}$	[56]
Gasifier	$Z = c'_{10} (\dot{m}_{Biomass})^{0.67} c'_{10} = 1600\$/(kg/h)^{0.67}$	[56]
Mixer	$Z = 0$	[61]
SRC Condenser	$Z = c'_{11} \dot{m} c'_{11} = 1773\$/(kg/s)$	[62]
SRC Turbine	$Z = c'_{12} \dot{W}_{ST}{}^{0.7} c'_{12} = 6000\$/(kW^{0.7})$	[62]
SRC Pump	$Z = c'_{13} \dot{W}_P{}^{0.71} c'_{13} = 3540\$/(kW^{0.71})$	[62]
Generator	$Z = c'_{14} (A_G/100)^{0.6} c'_{14} = 17500\$/(m^2)^{0.6}$	[63]
Absorber	$Z = c'_{15} (A_A/100)^{0.6} c'_{15} = 16000\$/(m^2)^{0.6}$	[63]
Rectifier	$Z = c'_{16} (A_R/100)^{0.6} c'_{16} = 17000\$/(m^2)^{0.6}$	[64]
ARC Condenser	$Z = c'_{17} (A_C/100)^{0.6} c'_{17} = 8000\$/(m^2)^{0.6}$	[63]
ARC Evaporator	$Z = c'_{18} (A_E/100)^{0.6} c'_{18} = 16000\$/(m^2)^{0.6}$	[63]
ARC HX.s	$Z = c'_{19} (A_H/100)^{0.6} c'_{19} = 16000\$/(m^2)^{0.6}$	[63]
ARC Valves	$Z = 0$	[63]
ARC Pump	$Z = c'_{20} \dot{W}_P{}^{0.8} c'_{20} = 1120\$/(kW^{0.8})$	[31]
ORC Condenser	$Z = c'_{21} (A_C)^{0.6} c'_{21} = 516.62\$/(m^2)^{0.6}$	[65]
ORC Turbine	$Z = c'_{22} \dot{W}_T{}^{0.75} c'_{22} = 4750\$/(kW^{0.75})$	[65]
ORC Pump	$Z = c'_{23} \dot{W}_{ST}{}^{0.65} c'_{23} = 200\$/(kW^{0.65})$	[65]
ORC2 Condenser (air-cooled) — Condenser	$Z = c'_{24} (A_C/200)^{0.89} c'_{24} = 156000\$/(m^2)^{0.89}$	[28]
ORC2 Condenser (air-cooled) — Fan	$Z = c'_{25} (\dot{W}_F/50)^{0.76} c'_{25} = 12300\$/(kW^{0.76})$	[28]

where C_{ei} is the exergoenvironmental impact coefficient [60,66]:

$$C_{ei} = \frac{1}{\psi_{ex}} \tag{79}$$

The exergoenvironmental impact improvement, which shows the positive effects of the system on the environment, is calculated as [60,66]:

$$\theta_{eii} = \frac{1}{\theta_{ei}} \tag{80}$$

The exergy stability factor is obtained by [60,66]:

$$f_{es} = \frac{\dot{E}x_{D,Tot}}{\dot{E}x_{D,Tot} + \dot{E}x_{out} + 1} \tag{81}$$

The unit emission of carbon dioxide which is the ratio of emitted CO_2 to the production rate of the system considered as an environmental factor, and is defined as follows [7,49]:

$$EMI_{CO_2} = \frac{\dot{m}_{CO_2,emitted}}{\dot{W}_{net} + \dot{Q}_{Heating} + \dot{m}_{H_2} LHV_{H_2} + \dot{m}_{water} h_{water}} \times 3600 \tag{82}$$

4. Validation

The model has been validated for different subsystems of the plant to confirm the correctness of the obtained results. Considering that the whole system is a collection of several subsystems, each has been validated separately using the modeling code developed in the EES software. The conditions and assumptions are adjusted to compare with those reported in the references.

The experimental work of Loha et al. [39] has been used to validate the steam gasification process. For this purpose, the syngas composition has been compared and presented in Table 5. The results obtained from this process modeling show a good agreement with their experimental results. The biogas-fueled Brayton cycle has been verified by reproducing the results of Zhang et al. [38]. The comparison of the obtained results with those available in that work, which is given in Table 6, shows the accuracy of the modeling. Table 7 shows the validation performed for the ammonia-water absorption unit. Comparing important obtained results with Adewusi's [67] model results indicates that the developed code is reliable. Validation of steam and organic Rankine cycles has been done by reproducing the results of Refs. [27,31], and the results are compared in Tables 8-9. The results presented in these tables also indicate the accuracy of the modeling.

Therefore, the validity of the overall system modeling is corroborated due to the correctness of the results obtained from the modeling of the subsystems.

5. Case study – Çiğli WWTP – Izmir

The proposed multigeneration system is fed from the sewage sludge of Çiğli wastewater treatment plant. Çiğli with the GPS coordinates of 38°29′N and 27°3′E, is a metropolitan district of Izmir Province in Turkey. The diagrams of the Çiğli hourly variations of average ambient temperature and relative humidity are presented in Fig. 8 [68]. This region's average temperature and relative humidity are 18.11 °C and 60.05%, respectively. Moreover, the highest and lowest ambient temperatures are associated with July (41 °C) and January (-6°C). Meanwhile, the relative humidity is maximum (100%) in the beginning and the end months of the year and is minimum (11%) in June. Also, as expected, the diagrams indicate that temperature and relative humidity are inversely related. The air is more humid at low temperatures, and at high temperatures, the air is drier.

Çiğli WWTP was built to save the Gulf of Izmir from sewage pollution. This WWTP is located south of Kaklıç airport in the former Gediz delta. It is built on a land area of 300,000 m^2, and the average capacity of

this plant is about 600,000 m^3 per day. In 2019, 190 million m^3 of wastewater was treated in this treatment plant [69].

6. Results and discussion

The mentioned multigeneration system, which is provided for the production of power, freshwater, hydrogen, and heating, is modeled by EES software. The schematic of this system was presented in Fig. 2 previously. This system feeds with the wet sewage sludge from the wastewater treatment plant. The characteristics of wet sewage sludge before and after anaerobic digestion are presented in Table 10. Input data for the plant modeling is provided in Table 11.

The main modeling results for this system in the mentioned base case condition are presented in Table 12. As can be seen, the system's overall energy and exergy efficiencies are 35.48% and 40.18%, respectively. In addition, this system can produce 18.42 L of freshwater and 3180 kg of hydrogen per hour. According to the information obtained from Çiğli WWTP, the annual energy consumption of this WWTP is equal to 44847.08 MWh, and from the results reported in Table 12, this system can generate 142,000 MWh energy annually, about 3.1 times the needs of Çiğli WWTP.

Thermodynamic properties including mass flow rate($\dot{m}$), temperature (T), pressure (P), the ammonia concentration in the refrigeration cycle (x), and the total exergy rate ($\dot{E}x$) for the base case conditions, are reported in Table 13.

Section 2 (System description) it was explained that the system integration is completed in six steps by adding different subsystems. The following will show how moving towards multigeneration improves system performance from energy, exergy, and environmental perspectives.

Energy efficiency, exergy efficiency, and exergetic performance coefficient variation during system integration in six steps are shown in Fig. 9. As can be seen, the energy and exergy efficiencies increase steadily, so that reaching from 15.32% and 17.24% in the first step to 35.48% and 40.18% in the last step of system formation, respectively. However, the exergetic performance coefficient has a drop in the third step of system completion and then increases again. The reason is that the equipment with the highest exergy destruction contribution is added to the system at this step.

The variation of the exergoenvironment factor, environmental damage effectiveness factor, exergy stability factor, and the unit emission of carbon dioxide during system integration in six steps are shown in Fig. 10. These changes are slightly fluctuating. Still, in a general view, it can be concluded that this integration favors the system. The environmental factors in the last step of completing the system improve more than the first steps.

Fig. 11 shows the contribution of subsystems in the total exergy destruction rate of the whole system and the contribution of components in the exergy destruction rate of the subsystem with the highest share. The Biomass conversion subsystem has the largest contribution among other subsystems, and the contribution of the atmospheric water harvesting unit is very small. Also, the gasifier with a share of 57.75%, has the highest exergy destruction rate among other components.

The moisture content of Biomass, steam to Biomass ratio, and gasification temperature are three important factors affecting the lower heating value and molar fraction of wet syngas components. Fig. 12 shows the impact of these three factors on the mole fraction of components and LHV of the syngas. As shown in this figure, in the given range of variables, by increasing the moisture content and steam to Biomass ratio, the H_2O mole fraction grows. In contrast, the lower heating value and molar fraction of other constituents decrease. Meanwhile, increasing the gasification temperature in the given range decreases the H_2O mole fraction, and the lower heating value grows.

As mentioned earlier, the gasifier has the largest share in the exergy destruction rate of the system. Therefore, a parametric study was conducted on three essential factors on the exergy destruction rate of the gasifier. As shown in Fig. 13, increasing the steam to Biomass ratio decreases the exergy destruction rate because of the increase of $\dot{m}_{15}$ and $\dot{m}_{16}$ and the much higher exergy value of stream 16 compared to stream 15. On the other hand, increasing the gasifier temperature and Biomass moisture content increases the exergy destruction rate of the gasifier. This increase can be easily justified with the help of the gasifier's exergy

Table 5
The steam gasification produced gas composition vs. the experimental results.

Dry Syngas	Present work	Loha experimental data [39]	RMS
H_2(%)	49.19	49.50	1.2478
CO(%)	23.71	23.70	
CO_2(%)	23.09	21.20	
CH_4(%)	4.00	5.60	

Input values: $T_g = 750$ °C, $MC_B = 0.0995$, $CH_{0.92}O_{0.71}$, steam/Biomass = 1.

Table 6
Validation of the biogas-fueled Brayton cycle modeling.

State	T (K)		P (bar)		$\dot{m}$(kg/s)	
	Result	Ref. [38]	Result	Ref. [38]	Result	Ref. [38]
15	298.2	298.15	1.013	1.013	4.77	4.77
16	612.2	612.65	10.23	10.23	4.77	4.77
17	650	650	9.72	9.72	4.77	4.77
18	1250	1250	9.33	9.23	4.935	4.96
19	824.8	822.65	1.16	1.12	4.935	4.96
20	788.7	789.15	1.10	1.07	4.935	4.96

Input values: CPR = 0.1, $T_{17} = 377$ °C, $T_{18} = 977$ °C, $\dot{m}_{air} = 4.77$ kg/s.

Table 7
Validation of the ammonia–water absorption system.

Parameter	Present work	Adewusi model data [67]
COP	0.624	0.598
Q_{gen} (kW)	265.1	267.9
Q_{abs} (kW)	233.3	231
Q_{rec} (kW)	44.7	50.7
Q_{cond} (kW)	157.4	151
Q_{eva} (kW)	167.3	162

Input values: $T_{evap} = -10$ °C, $\dot{m} = 1$ kg/s, $T_{condenser} = 40$ °C, $T_{absorber} = 40$ °C, $\Delta x = 0.10$, ammonia-water strong solution = 99.96%, $\eta_{pump} = 50\%$, $\varepsilon_{SHX} = 100\%$, $\varepsilon_{CEHX} = 95\%$.

Table 8
Validation of the steam Rankine cycle.

Parameter	Present work	Ref. [31]
W_{net} (kW)	2789	2789
η_{en} (%)	15.64	15.2

Input values: TIT = 420 °C, $\dot{m} = 6.44$ kg/s, TIP = 8000 kPa, $P_{cond} = 100$ kPa, $\eta_{pump} = 90\%$, $\eta_{turbine} = 85\%$, $\eta_{mec,turbine} = 90\%$.

Table 9
Validation of the organic Rankine cycle.

Parameter	Present work	Ref. [27]
W_{net} (kW)	2450	2458
η_{en} (%)	24.94	25.0

Input values: $\eta_{pump} = 90\%$, $\eta_{turbine} = 85\%$. ORC1(Cyclohexane): $\dot{m} = 13$ kg/s, TIT = 300 °C, TIP = 3000 kPa, $P_{cond} = 100$ kPa. ORC2(Isobutane): $\dot{m} = 5$ kg/s, TIP = 3000 kPa, $P_{cond} = 100$ kPa.

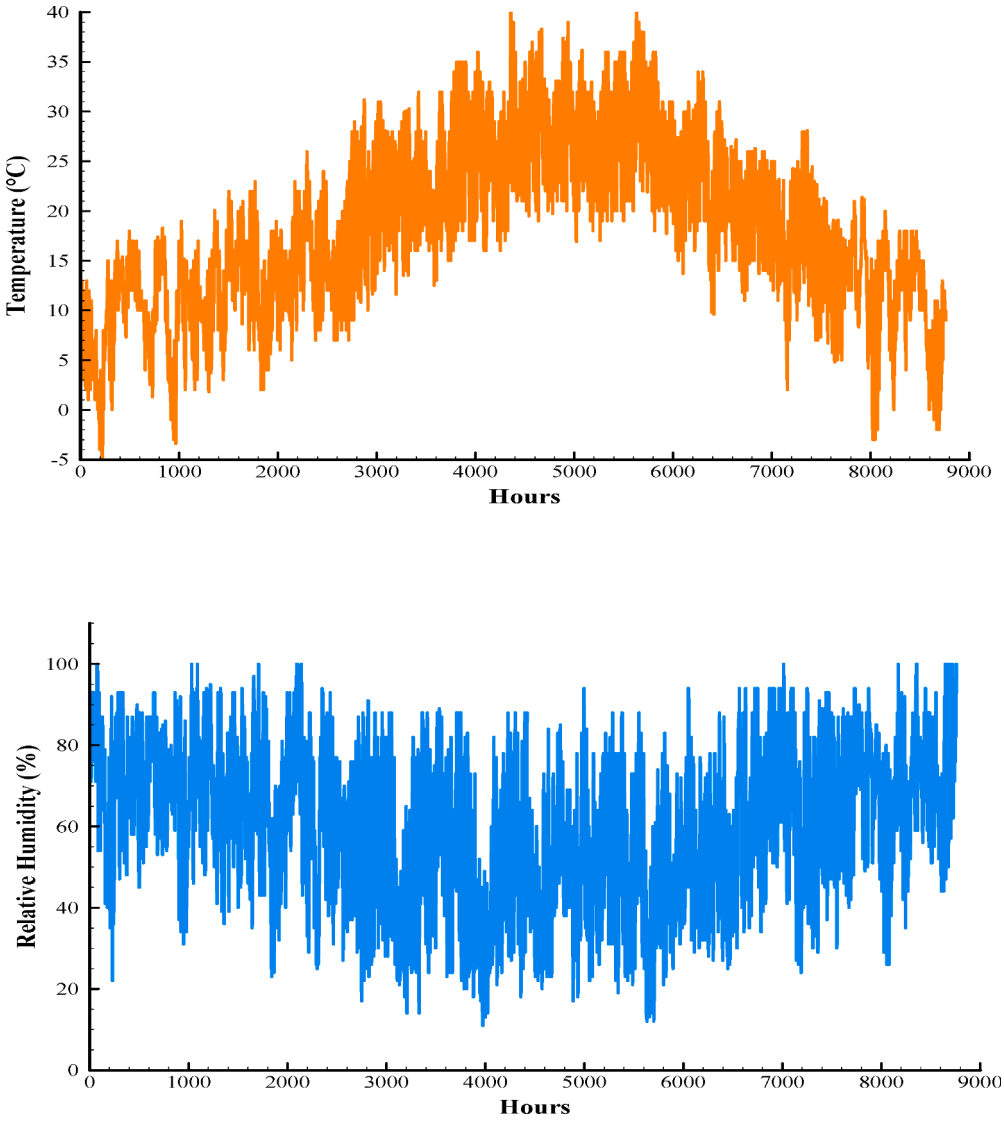

Fig. 8. The hourly variations of average ambient temperature and relative humidity of Çiğli.

Table 10
Proximate and ultimate analysis of sewage sludge [70].

Biomass	Proximate analysis (wt% /wt.)			Ultimate analysis (db, wt% /wt.)				
	Moisture content	Volatile matter	Ash	C	H	O	N	S
Raw sludge	75	65	30	37	4.5	19.5	3.3	0.65
Digestate	75	50	40	33.5	2.5	12.5	1.1	0.40

and energy equations mentioned in Table 2. The growth of the exergy destruction rate at the end of moisture content increasing is faster than its beginning, but the increase of the destruction rate with the rise in gasification temperature goes through an approximately linear trend. Regarding the steam to Biomass ratio, it is the case that the reduction of the exergy destruction rate of the gasifier at the end of STBM increasing is slower than its beginning.

The effect of key variables of the Brayton cycle, absorption refrigeration cycle, steam Rankine cycle, and organic Rankine cycle on their efficiency are shown in Fig. 14. As can be seen, increasing the pressure ratio of the gas turbine improves the performance of the Brayton cycle, while increasing the pressure ratio of the air compressor reduces the efficiency of the cycle. In the absorption refrigeration cycle, the effect of the temperature of the absorber and condenser as key factors have been evaluated on the cycle coefficient of performance. It can be seen that the increase of both factors caused a decrease in the performance criteria of this cycle. In the steam Rankine cycle, turbine inlet pressure and inlet temperature factors are directly proportional to cycle efficiencies. In the organic Rankine cycle, the effect of the first and second cycles' turbine inlet pressure on the cycle performance was evaluated. The efficiency

Table 11
Input data for system modeling.

Parameter	Value	Units
Anaerobic Digestion [14,30,35]		
Sewage sludge flow rate	1.88	kg/s
LHV of sludge	18,000	kJ/kg
LHV of digestate	14,500	kJ/kg
Digestion temperature (mesophilic)	35	°C
Digestion pressure	101.3	kPa
Amount of destruction in the digester	70	%
Work needed for the digestion	0	W
Biomass simplified chemical formula	$C_{13.08}H_{18.95}O_{5.17}$	–
Brayton Cycle [30]		
Pressure ratio of the compressors	10	–
Isentropic efficiency of the fuel compressor	85	%
Isentropic efficiency of the air compressor	85	%
Combustion Chamber inlet temperature	576.85	°C
Turbine inlet temperature	1246.85	°C
Pressure ratio of the gas turbine	8.3	–
Isentropic efficiency of the gas turbine	85	%
Steam Gasification [19,71]		
Temperature of the inlet Biomass	35	°C
Temperature of the inlet steam	400	°C
Temperature of the outlet syngas	800	°C
Gasification pressure	101.3	kPa
Steam to Biomass ratio	1	–
Biomass simplified chemical formula	$CH_{0.89}O_{0.28}$	–
Water-Gas Shift Reaction Unit		
Temperature of the inlet steam	200	°C
Temperature of the produced hydrogen	25	°C
Steam Rankine Cycle [31]		
Steam flow rate in the cycle	12	kg/s
Turbine inlet temperature	420	°C
Turbine inlet pressure	8000	kPa
Turbine outlet pressure	100	kPa
Isentropic efficiency of the pump	90	%
Isentropic efficiency of the steam turbine	85	%
Organic Rankine Cycle1 [27]		
Working fluid	Cyclohexane	
Fluid flow rate in the cycle	13	kg/s
Turbine inlet temperature	300	°C
Turbine inlet pressure	3000	kPa
Turbine outlet pressure	100	kPa
Isentropic efficiency of the pump	90	%
Isentropic efficiency of the steam turbine	85	%
Organic Rankine Cycle2 [27]		
Working fluid	Isobutane	
Fluid flow rate in the cycle	5	kg/s
Turbine inlet pressure	3000	kPa
Turbine outlet pressure	100	kPa
Isentropic efficiency of the pump	90	%
Isentropic efficiency of the steam turbine	85	%
Absorption Refrigeration Cycle [67]		
Isentropic efficiency of the pump	90	%
Effectiveness of solution heat exchanger	100	%
Effectiveness of condensate precooler	95	%
Evaporator temperature	−10	°C
Condenser temperature	40	°C
Absorber temperature	40	°C
Mass flow rate of water	1	kg/s
Ammonia-water strong solution	99.96	%
Atmospheric Water Harvesting [46]		
Relative humidity of inlet air	40	%
Relative humidity of exit air	100	%
Temperature of inlet air	25	°C

Table 12
Some of the main results.

Energy	Exergy	Exergoeconomic	Exergoenvironment
$\eta_{BC} = 21.71\%$	$\psi_{BC} = 31.24\%$	$\dot{Z}_{total} = 1.949 M\$/Year$	$f_{ei} = 0.594$
$\eta_{SRC} = 26.07\%$	$\psi_{SRC} = 41.66\%$	$\dot{C}_f = 6.978 M\$/Year$	$\theta_{ei} = 1.478$
$\eta_{ORC} = 24.80\%$	$\psi_{ORC} = 46.46\%$	$\dot{C}_{env} = 7.647 M\$/Year$	$C_{ei} = 2.489$
$\eta_{WGSRU} = 20.95\%$	$\psi_{WGSRU} = 87.31\%$	$\dot{C}_Q = 55.36 M\$/Year$	$\theta_{eii} = 0.6764$
$COP_{en,ARC} = 62.67\%$	$COP_{ex,ARC} = 12.73\%$	$\dot{C}_{D,TOTAL} = 30.31 M\$/Year$	$f_{es} = 0.5383$
$\eta_{Overall} = 35.48\%$	$\psi_{Overall} = 40.18\%$	$\dot{C}_{TOTAL} = 102.2 M\$/Year$	$EMI_{CO_2} = 0.2327 t/MWh$
$\dot{Q}_{Gas} = 173 MW$	$\dot{E}x_{D,Tot} = 146170 kW$	$c_{p,TOTAL} = 13.05\$/GJ$	
$\dot{W}_{net} = 17750 kW$			
$\dot{Q}_{Heating} = 47440 kW$			
$WGR = 18.42 l/h$			
$\dot{m}_{H_2} = 3180 kg/h$			

increasing with the inlet pressure of the first turbine experiences a maximum point in its path, that is, up to a pressure of 3800 kPa, energy and exergy efficiencies of this cycle increase and then decrease. While increasing the inlet pressure of the second turbine is entirely beneficial to cycle efficiencies.

Two key factors affecting atmospheric water harvesting are temperature and relative humidity. The effect of these two variables on the water generation rate and the amount of power consumption is presented in Fig. 15. The amount of water generation in all relative humidity increases with the air temperature. The dew point of water vapor increases with growing air temperature, so the water production rate is higher in higher temperatures. As the relative humidity increases, water vapor density in humid air increases. Consequently, as the density of water vapor in humid air increases, the dew point of moist air increases, which means less cooling power is required to condense the water vapor in moist air. The water production rate from this cycle can be determined by having the relative humidity and the air temperature. Therefore, these curves are named device performance curves.

The products of this multigeneration system are electrical power, heating, hydrogen, and freshwater. The production rate of these products in the base case condition was presented in Table 12. Fig. 16 shows the variation of electrical power, heating, and hydrogen production rates as a function of the input feed rate. As can be seen, increasing the Biomass feed rate from 6 to 11 kg/s increases the production rate of these products from 16,404 to 20833 kW, from 34,048 to 78062 kW, and from 0.70 to 1.29 kg/s, respectively.

The amount of water production rate in the different months of the year is shown in Fig. 17. The maximum generation rate is for October with 38.67 l/h, and the minimum is for June with 24.6 l/h freshwater production. As shown in this figure, the generation rate in the autumn season is better than the others.

The effect of Biomass flow rate and gasification temperature on the system's overall efficiency and the unit emission of carbon dioxide is presented in Fig. 18. Evaluations show that the feed rate increasing from 6 to 11 kg/s improves the energy efficiency by 0.91%, and reduces the unit emission of carbon dioxide by approximately 6 kg/MWh. Nevertheless, it causes exergy efficiency reduction (because of enhancing the total exergy destruction rate of the system). On the other hand, increasing the temperature of the gasifier is beneficial to the system in terms of these three criteria. Increasing the gasification temperature from 520 to 820 °C improves the energy and exergy efficiencies by 16.58% and 17.3%, respectively, and reduces the unit emission of carbon dioxide by about 135 kg/MWh. This is mainly due to the increased hydrogen production rate by the rising gasification temperature.

The contribution of the capital investment cost of subsystems is shown in Fig. 19. As can be seen, Rankine cycles have the highest capital investment cost among the other subsystems. In both cycles, turbines have the highest share. After that, in the steam Rankine cycle, the largest share is for the pump, and in the organic Rankine cycle, the largest share is for the air-cooled condenser. In addition, as concluded in previous studies [72], this figure also shows that the capital investment cost of the

Table 13
Properties of the system state points.

Stream	Fluid	$\dot{m}(kg/s)$	T℃	$P(kPa)$	x	$E\dot{x}(MW)$
1	Raw sewage sludge	7.52	25	101.3	–	0
2	Digestated sewage sludge	6.335	35	101.3	–	121.125
3	Biogas	1.185	35	101.3	–	82.496
4	Biogas	1.185	247.9	1013	–	20.973
5	Water	0.939	25	101.3	–	21.321
6	Water	0.939	85	101.3	–	0.046
7	Air	20.92	25	101.3	–	0.067
8	Air	20.92	341.3	1013	–	0
9	Air	20.92	576.9	962.4	–	6.379
10	Combustion Products	22.1	1247	914.2	–	9.489
11	Combustion Products	22.1	750	110.1	–	24.565
12	Combustion Products	22.1	544.9	106.8	–	9.867
13	Combustion Products	22.1	534.6	106.8	–	6.142
14	Combustion Products	22.1	525.5	106.8	–	5.973
15	Steam	25.32	400	101.3	–	5.825
16	Syngas	31.66	800	101.3	–	32.028
17	Steam	31.66	200	101.3	–	155.013
18	Hydrogen	0.883	25	101.3	–	33.959
19	WGSRU products	62.44	581.5	101.3	–	103.411
20	Ammonia/ water	1	40	286.8	0.3964	70.560
21	Ammonia/ water	1	40.13	1556	0.3964	7.900
22	Ammonia/ water	1	104.5	1556	0.3964	7.902
23	Ammonia/ water	0.857	124.2	1556	0.2964	7.948
24	Ammonia/ water	0.857	40.13	1556	0.2964	5.128
25	Ammonia/ water	0.857	40.39	286.8	0.2964	5.078
26	Ammonia/ water	0.152	101.9	1556	0.9583	5.077
27	Water	0.010	101.9	1556	0.3964	2.963
28	Ammonia	0.142	44.07	1556	0.9996	0.083
29	Ammonia	0.142	40	1556	0.9996	2.873
30	Ammonia	0.142	10.29	1556	0.9996	2.865
31	Ammonia	0.142	−10.33	286.8	0.9996	2.865
32	Ammonia	0.142	−10	286.8	0.9996	2.864
33	Ammonia	0.142	36.71	286.8	0.9996	2.842
34	Air	9.839	25	101.3	–	2.841
35	Air	9.834	9.476	101.3	–	0
36	Water	0.005	9.476	101.3	–	0.004
37	Flue gas	84.55	572	102.4	–	0.00026
38	Flue gas	84.55	348	102.4	–	76.086
39	Flue gas	84.55	278.4	102.4	–	55.312
40	Flue gas	84.55	110	102.4	–	50.069
41	Water	12	100.4	8000	–	40.733
42	Water	12	420	8000	–	0.504
43	Water	12	99.63	100	–	15.317
44	Water	12	99.63	100	–	5.317
45	Cyclohexane	13	81.44	3000	–	0.403
46	Cyclohexane	13	300	3000	–	0.174
47	Cyclohexane	13	219.9	100	–	3.841
48	Cyclohexane	13	80.31	100	–	1.875
49	Cyclohexane	13	80.31	100	–	0.846
50	Isobutane	5	−10.69	3000	–	0.121
51	Isobutane	5	183.5	3000	–	0.300
52	Isobutane	5	91.64	100	–	0.931
53	Isobutane	5	−12.01	100	–	0.058
54	Water	3.762	25	101.3		0.276
55	Water	3.762	35	101.3		0.187
56	Water	1.068	25	101.3		0.190
57	Water	1.068	35	101.3		0.053
58	Water	5.551	25	101.3		0.054
59	Water	5.551	35	101.3		0.277
60	Water	97.75	25	101.3		0.281
61	Water	97.75	85	101.3		4.882
62	Water	110.7	25	101.3		7.063
63	Water	110.7	35	101.3		5.531
64	Air	91.62	−20	101.3		5.607
65	Air	91.62	10	101.3		0.347
66	Water	91.19	25	101.3		0.035
67	Water	91.19	85	101.3		4.555

air-cooled condenser is significantly higher than that of water-cooled condensers.

Fig. 20 demonstrates the contribution of the subsystem's cost rates of exergy destruction. Considering that this factor is obtained from the product of the cost of the fuel stream for a component and its exergy destruction rate, the distribution shown in this figure can be justified with the help of Fig. 11. Biomass conversion subsystem has the largest share of exergy destruction rate and cost rates of exergy destruction.

The column chart for comparing the exergoeconomic factor of all equipment is shown in Fig. 21. According to this diagram, the highest value of the exergoeconomic factor is for the air-cooled condenser of ORC2 and the solution heat exchanger of ARC. That is, this equipment's capital investment cost is higher than the cost of exergy destruction. Therefore, it is better to replace these components with lower equipment cost to improve the system's economic performance.

The effect of gasification temperature on the total cost rate of the system, the unit cost of total products, and the unit cost of electricity and hydrogen products are investigated. As shown in Fig. 22, Increasing the gasification temperature within the specified range causes an increase in the total cost rate of the system. As discussed earlier, increasing the temperature of the gasifier raises its exergy destruction rate and its heat requirement. According to Eq. (69), these factors increase the total cost rate of the system. On the other hand, although increasing the gasification temperature increases the production rate of hydrogen, it increases the cost of its production, which is mainly due to the high cost spent on supplying heat to the gasifier. Utilizing waste heat sources seems more suitable for providing the heating power required by the gasifier.

7. Conclusions

A new urban sewage sludge-based multigeneration system for power, heating, hydrogen, and freshwater production was developed and evaluated from the energy, exergy, exergoeconomic, and exergoenvironment points of view. A case study for Çiğli wastewater treatment plant has been conducted on this system, and parametric studies have been performed to investigate the effect of the main parameters on the system's performance criteria. Some of the main outcomes of this study are listed below:

- This system's energy and exergy efficiencies obtained 35.48% and 40.18%, respectively.
- The gasifier has the largest share (57.75%) of the exergy destruction rate among the other components.
- Multigeneration has improved the system's performance so that the energy and exergy efficiencies have been improved by 20.16% and 22.94%, respectively, compared to the single-generation main system. Also, it has reduced the unit emission of carbon dioxide by about 4 times.
- The exergoenvironment, environmental damage effectiveness, and exergy stability factors of the proposed system obtained 0.4684, 1.166, and 0.5383, respectively.
- The hydrogen production rate in the base case conditions is 3180 kg/h, and its unit cost of production is 12.58 $/GJ.

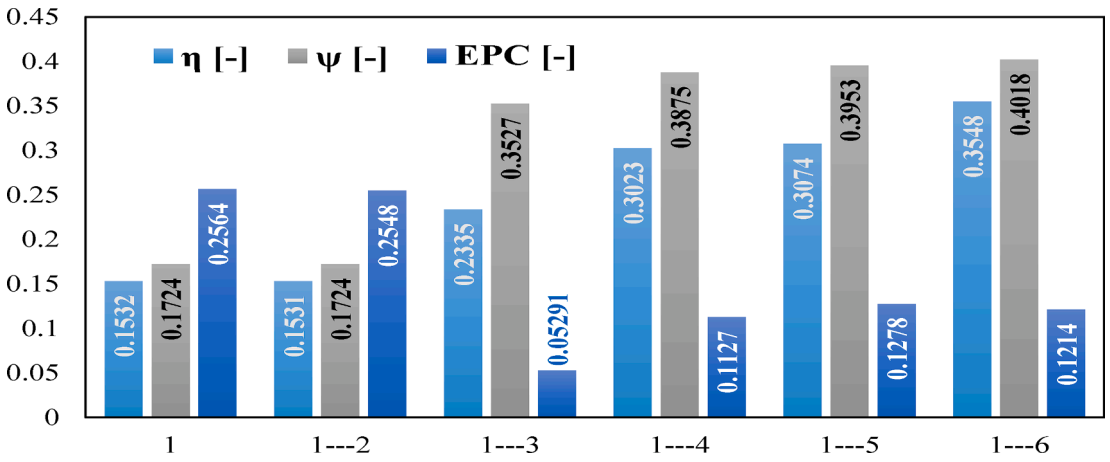

Fig. 9. Energy efficiency (η), exergy efficiency (ψ), and exergetic performance coefficient (*EPC*) variation during system integration in six steps.

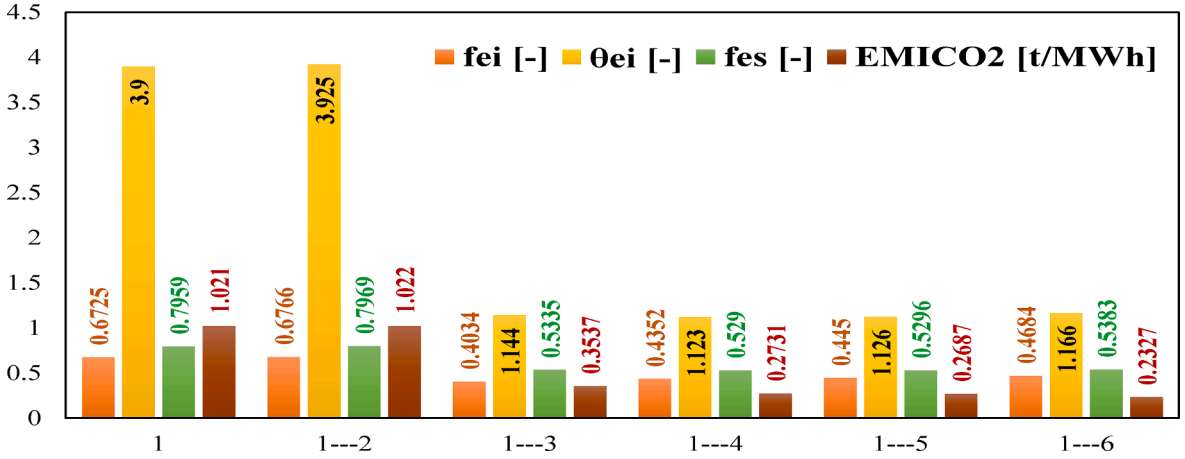

Fig. 10. Exergoenvironment factor (f_{ei}), the environmental damage effectiveness factor (θ_{ei}), exergy stability factor (f_{es}), and unit emission of carbon dioxide (EMI_{CO_2}) variation during system integration in six steps.

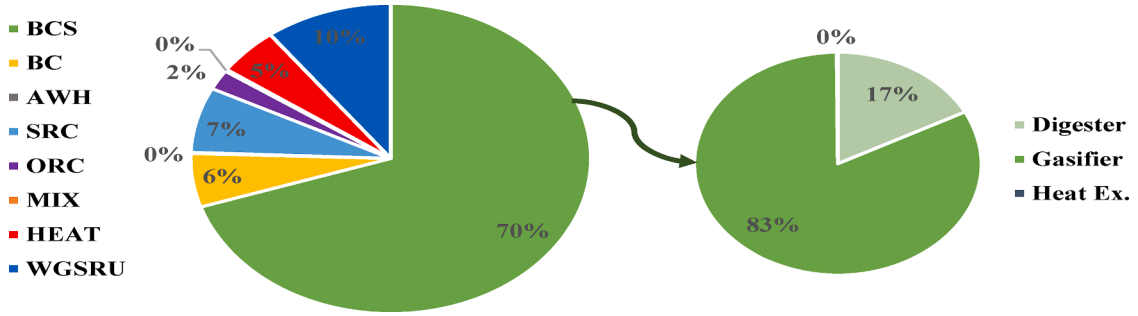

Fig. 11. The Contribution of exergy destruction rate of subsystems ($\dot{E}x_{D,sub,sys}$).

- The net power generation of the system is 17750 kW. This amount of electricity generation, in addition to supplying the electricity demand of Çiğli WWTP, can produce twice of surplus electricity that can be used during peak hours or sold.
- This system can produce more than 18 L of freshwater per hour in defined base case conditions. However, if the actual data of the studied area be used, it will be able to produce at least 24 l/h of freshwater.
- The total cost rate of the system and the unit cost of total products are calculated as 102.2 M$/Year and 13.05 $/GJ, respectively.
- Rankine cycles have the highest capital investment cost among the other subsystems.

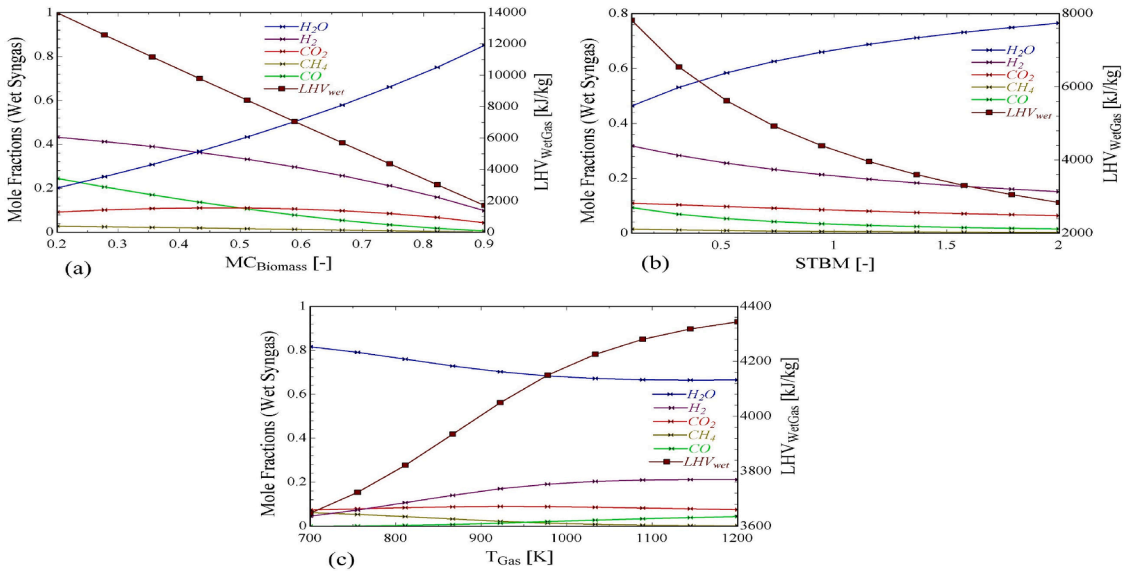

Fig. 12. The effect of a) moisture content of Biomass, b) steam to Biomass ratio, and c) gasification temperature on the constituents' mole fractions and lower heating value of the syngas.

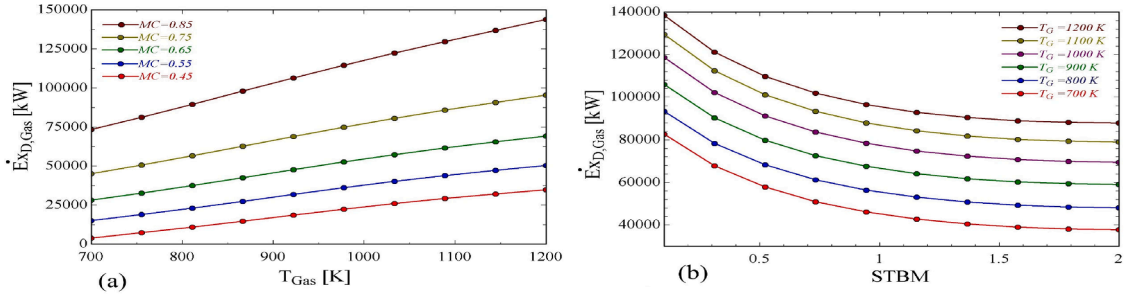

Fig. 13. The effect of a) gasification temperature, and b) steam to Biomass ratio on the exergy destruction rate of the gasifier.

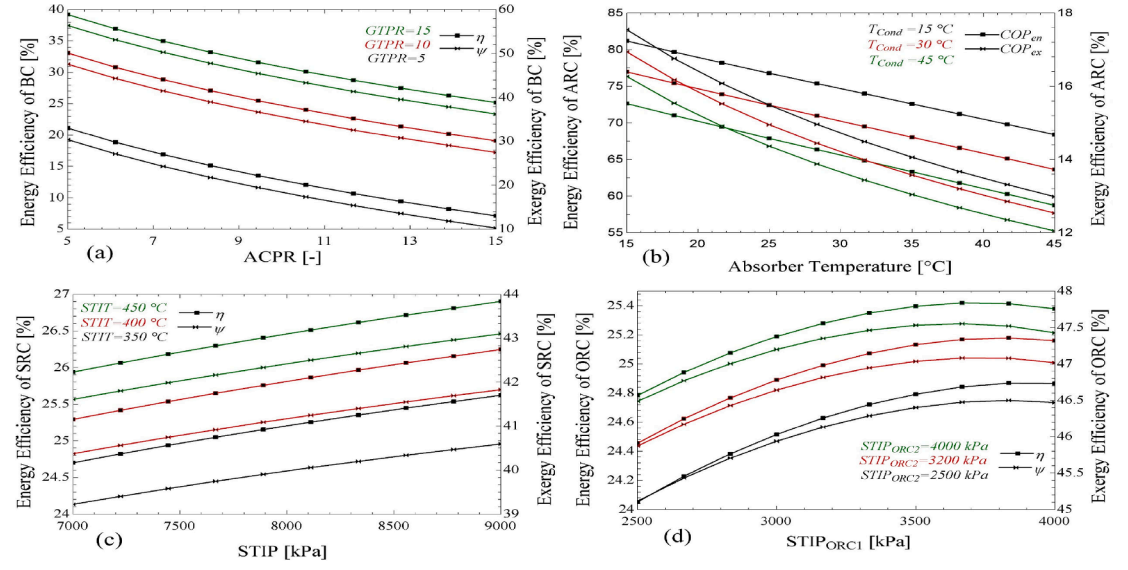

Fig. 14. The effect of key variables of BC, ARC, SRC, and ORC subsystems on their efficiency.

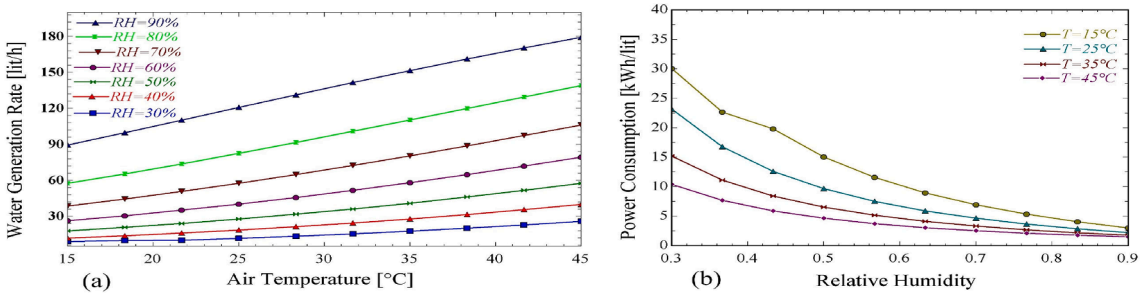

Fig. 15. The effect of ambient temperature and relative humidity on the a) water generation rate, and b) power consumption of AWH unit.

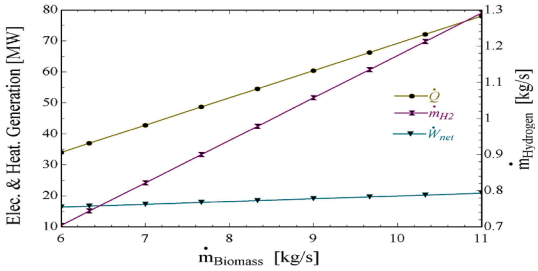

Fig. 16. The effect of the Biomass flow rate on the power, heating, and hydrogen generation rate.

- The results of parametric studies show that increasing the rate of Biomass improves the overall energy efficiency and production rates and also reduces the unit emission of carbon dioxide, but on the other hand, it causes a decrease in exergy efficiency and an increase in the unit cost of total products.
- The relative humidity of the air directly affects water production, so according to the parametric studies, increasing the relative humidity from 30% to 90% in a constant temperature (25 °C) increases the hourly water production rate from about 3 l/h to about 120 l/h.

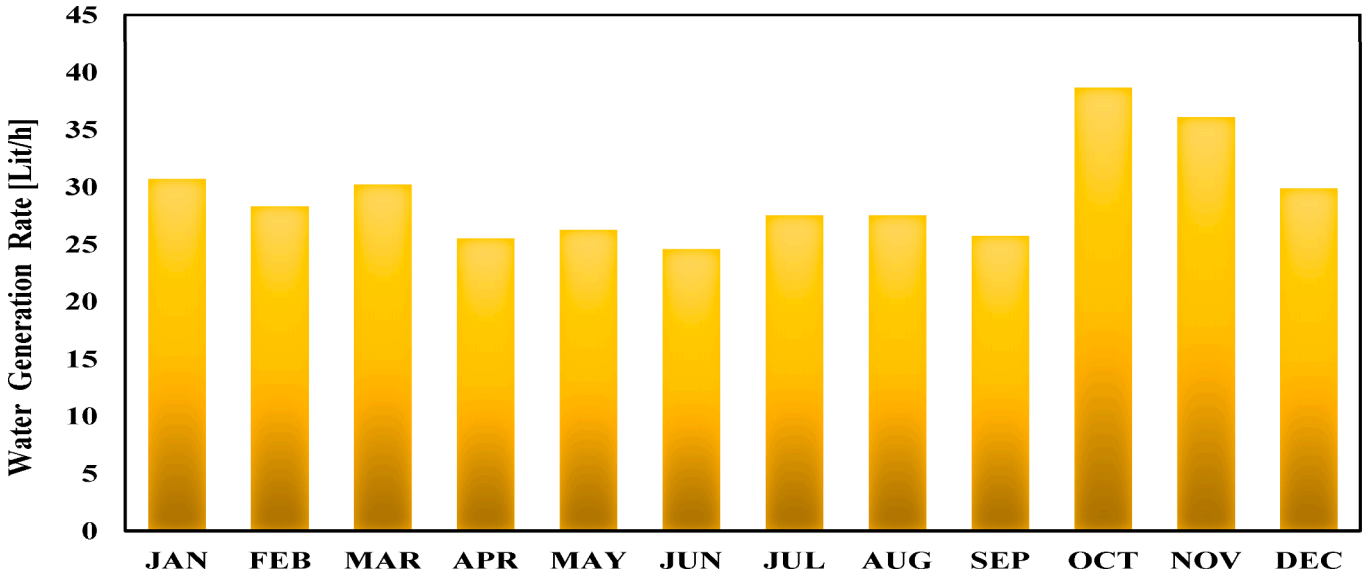

Fig. 17. Water generation rate along the year.

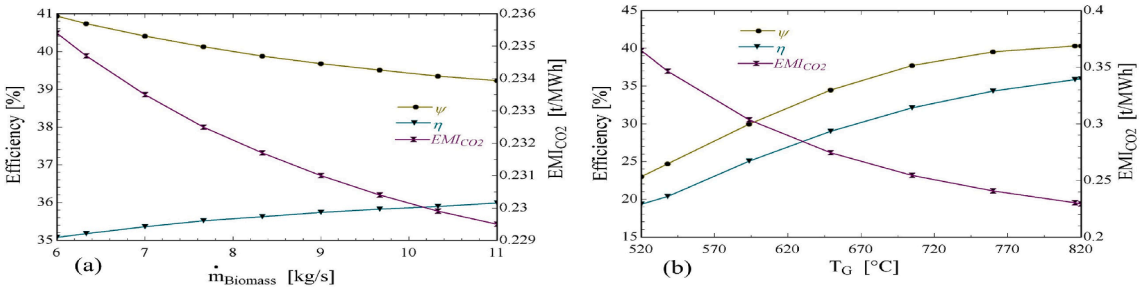

Fig. 18. The effect of a) Biomass flow rate and b) gasification temperature on the system overall efficiency and the unit emission of carbon dioxide.

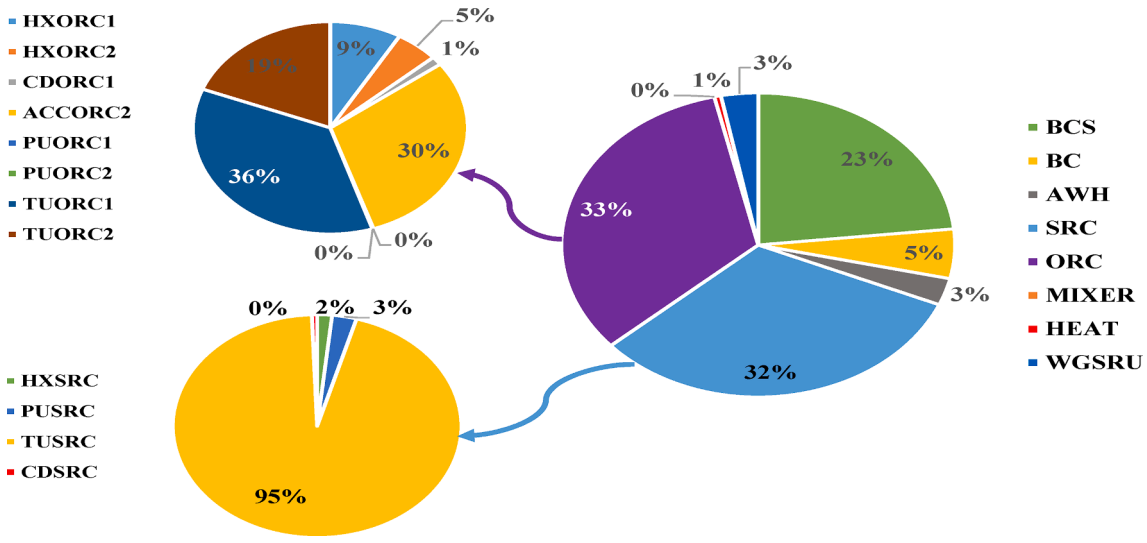

Fig. 19. Contribution of capital investment cost of subsystems ($\dot{Z}_{sub,sys}$).

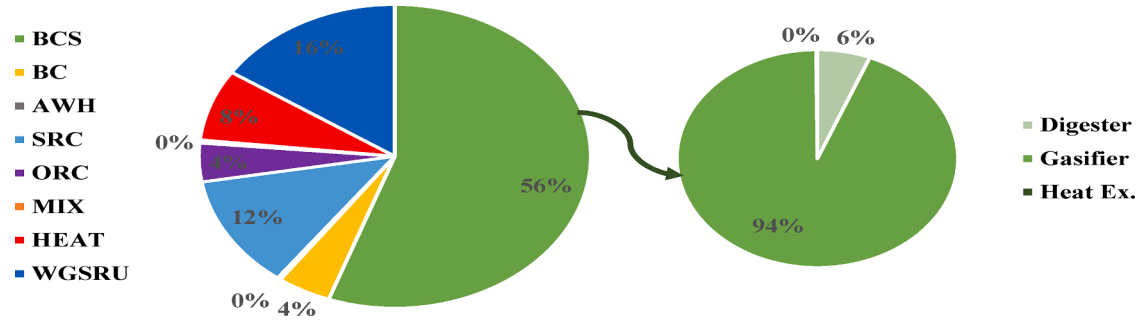

Fig. 20. Contribution of subsystem's cost rates of exergy destruction ($\dot{C}_{D,sub,sys}$).

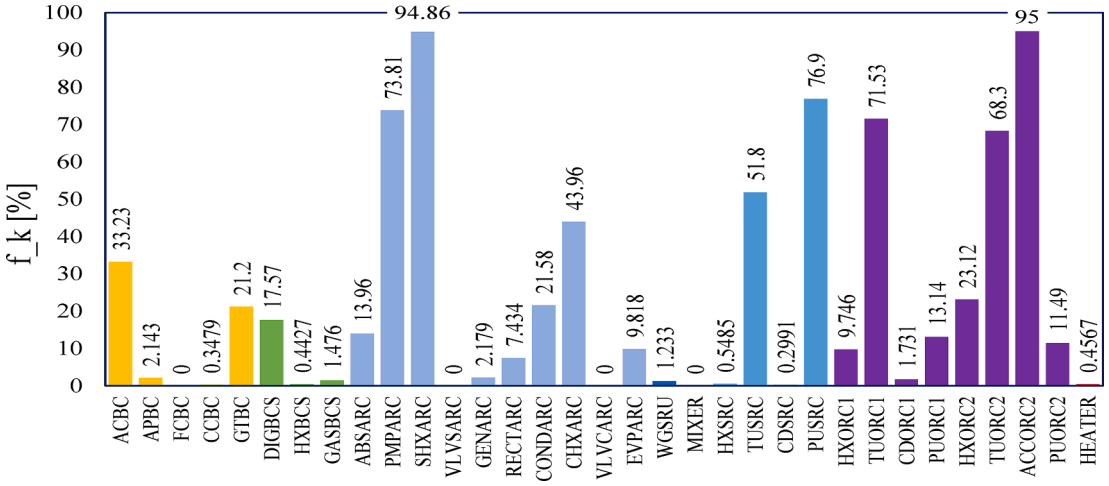

Fig. 21. Exergoeconomic factor for all components.

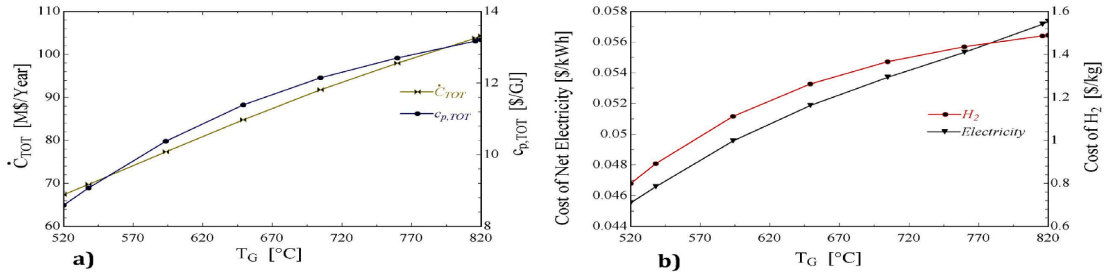

Fig. 22. The effect of gasification temperature on the a) total cost rate of the system and unit cost of total products, and b) unit cost of electricity and hydrogen products.

CRediT authorship contribution statement

Zahra Hajimohammadi Tabriz: Investigation, Conceptualization, Writing – original draft. **Mousa Mohammadpourfard:** Supervision, Conceptualization, Writing – review & editing. **Gulden G. Akkurt:** Writing – review & editing. **Saeed Zeinali Heris:** Writing – review & editing.

Declaration of Competing Interest

The authors declare that they have no known competing financial interests or personal relationships that could have appeared to influence the work reported in this paper.

Data availability

No data was used for the research described in the article.

Acknowledgment

This work was supported by the Scientific & Technological Research Council of Turkey under program of TUBITAK 2221 Fellowship.

References

[1] Ağbulut Ü, Sarıdemir S. A general view to converting fossil fuels to cleaner energy source by adding nanoparticles. Int J Ambient Energy 2021/10/03 2021,;42(13): 1569–74. https://doi.org/10.1080/01430750.2018.1563822.
[2] Dincer I, Acar C. Chapter 1.1 - Potential Energy Solutions for Better Sustainability. In: Dincer I, Colpan CO, Kizilkan O, editors. Exergetic, Energetic and Environmental Dimensions. Academic Press; 2018. p. 3–37.
[3] Abas N, Kalair A, Khan N. Review of fossil fuels and future energy technologies. Futures 2015/05/01/ 2015,;69:31–49. https://doi.org/10.1016/j.futures.2015.03.003.
[4] Raveesh G, Goyal R, Tyagi SK. Advances in atmospheric water generation technologies. Energ Conver Manage 2021/07/01/ 2021,;239:114226. https://doi.org/10.1016/j.enconman.2021.114226.
[5] Tu Y, Wang R, Zhang Y, Wang J. Progress and Expectation of Atmospheric Water Harvesting. Joule 2018/08/15/ 2018,;2(8):1452–75. https://doi.org/10.1016/j.joule.2018.07.015.
[6] Rong A, Lahdelma R. Role of polygeneration in sustainable energy system development challenges and opportunities from optimization viewpoints. Renew Sustain Energy Rev 2016/01/01/ 2016,;53:363–72. https://doi.org/10.1016/j.rser.2015.08.060.
[7] L. Khani, M. Mohammadpour, M. Mohammadpourfard, S. Z. Heris, and G. G. Akkurt, "Thermodynamic design, evaluation, and optimization of a novel quadruple generation system combined of a fuel cell, an absorption refrigeration cycle, and an electrolyzer," *International Journal of Energy Research,* https://doi.org/10.1002/er.7634 vol. 46, no. 6, pp. 7261-7276, 2022/05/01 2022, doi: https://doi.org/10.1002/er.7634.
[8] Khani L, Tabriz ZH, Mohammadpourfard M, Gökçen Akkurt G. Energy and exergy analysis of combined power, methanol, and light olefin generation system fed with shale gas. Sustain Cities Soc 2022/12/01/ 2022,;87:104214. https://doi.org/10.1016/j.scs.2022.104214.
[9] Ghiami S, Khallaghi N, Borhani TN. Techno-economic and environmental assessment of staged oxy-co-firing of biomass-derived syngas and natural gas. Energ Conver Manage 2021/09/01/ 2021,;243:114410. https://doi.org/10.1016/j.enconman.2021.114410.
[10] Yilmaz F, Ozturk M, Selbas R. Investigation of the thermodynamic analysis of solar Energy-Based multigeneration plant for sustainable multigeneration. Sustainable Energy Technol Assess 2022/10/01/ 2022,;53:102461. https://doi.org/10.1016/j.seta.2022.102461.
[11] Seiiedhoseiny M, Khani L, Mohammadpourfard M, Akkurt GG. Exergoeconomic analysis and optimization of a high-efficient multi-generation system powered by Sabalan (Savalan) geothermal power plant including branched GAX cycle and electrolyzer unit. Energ Conver Manage 2022/09/15/ 2022,;268:115996. https://doi.org/10.1016/j.enconman.2022.115996.
[12] Lak Kamari M, Maleki A, Daneshpour R, Rosen MA, Pourfayaz F, Alhuyi Nazari M. Exergy, energy and environmental evaluation of a biomass-assisted integrated plant for multigeneration fed by various biomass sources. Energy 2023/01/15/ 2023,;263:125649. https://doi.org/10.1016/j.energy.2022.125649.
[13] Safarian S, Unnthorsson R, Richter C. Hydrogen production via biomass gasification: simulation and performance analysis under different gasifying agents. Biofuels 2022/07/03 2022,;13(6):717–26. https://doi.org/10.1080/17597269.2021.1894781.
[14] Safari F, Dincer I. Development and analysis of a novel biomass-based integrated system for multigeneration with hydrogen production. Int J Hydrogen Energy 2019/02/05/ 2019,;44(7):3511–26. https://doi.org/10.1016/j.ijhydene.2018.12.101.
[15] Rulkens W. Sewage Sludge as a Biomass Resource for the Production of Energy: Overview and Assessment of the Various Options. Energy Fuel 2008/01/01 2008,; 22(1):9–15. https://doi.org/10.1021/ef700267m.
[16] Siddiqui O, Dincer I. Design and assessment of a new solar-based biomass gasification system for hydrogen, cooling, power and fresh water production utilizing rice husk biomass. Energ Conver Manage 2021/05/15/ 2021,;236: 114001. https://doi.org/10.1016/j.enconman.2021.114001.
[17] Ishaq H, Islam S, Dincer I, Yilbas BS. Development and performance investigation of a biomass gasification based integrated system with thermoelectric generators. J Clean Prod 2020/05/20/ 2020,;256:120625. https://doi.org/10.1016/j.jclepro.2020.120625.
[18] Ishaq H, Dincer I. A new energy system based on biomass gasification for hydrogen and power production. Energy Rep 2020/11/01/ 2020,;6:771–81. https://doi.org/10.1016/j.egyr.2020.02.019.
[19] Sotoodeh AF, Ahmadi F, Ghaffarpour Z, Ebadollahi M, Nasrollahi H, Amidpour M. Performance analyses of a waste-to-energy multigeneration system incorporated with thermoelectric generators. Sustainable Energy Technol Assess 2022/02/01/ 2022,;49:101649. https://doi.org/10.1016/j.seta.2021.101649.
[20] Yilmaz F, Ozturk M, Selbas R. Design and thermodynamic assessment of a biomass gasification plant integrated with Brayton cycle and solid oxide steam electrolyzer for compressed hydrogen production. Int J Hydrogen Energy 2020/12/09/ 2020,; 45(60):34620–36. https://doi.org/10.1016/j.ijhydene.2020.02.174.
[21] G. Onder, F. Yilmaz, and M. Ozturk, "Thermodynamic performance analysis of a copper–chlorine thermochemical cycle and biomass based combined plant for multigeneration," *International Journal of Energy Research,* https://doi.org/10.1002/er.5482 vol. 44, no. 9, pp. 7548-7567, 2020/07/01 2020, doi: https://doi.org/10.1002/er.5482.
[22] Ejeian M, Wang RZ. Adsorption-based atmospheric water harvesting. Joule 2021/07/21/ 2021,;5(7):1678–703. https://doi.org/10.1016/j.joule.2021.04.005.
[23] Chaitanya B, Bahadur V, Thakur AD, Raj R. Biomass-gasification-based atmospheric water harvesting in India. Energy 2018/12/15/ 2018,;165:610–21. https://doi.org/10.1016/j.energy.2018.09.183.
[24] Patel J, Patel K, Mudgal A, Panchal H, Sadasivuni KK. Experimental investigations of atmospheric water extraction device under different climatic conditions. Sustainable Energy Technol Assess 2020/04/01/ 2020,;38:100677. https://doi.org/10.1016/j.seta.2020.100677.
[25] Salek F, Eshghi H, Zamen M, Ahmadi MH. Energy and exergy analysis of an atmospheric water generator integrated with the compound parabolic collector with storage tank in various climates. Energy Rep 2022/11/01/ 2022,;8:2401–12. https://doi.org/10.1016/j.egyr.2022.01.178.
[26] Tabriz ZH, Khani L, Mohammadpourfard M, Akkurt GG. Biomass driven polygeneration systems: a review of recent progress and future prospects. Process Saf Environ Prot 2022/11/15/ 2022,. https://doi.org/10.1016/j.psep.2022.11.029.
[27] Almahdi M, Dincer I, Rosen MA. A new solar based multigeneration system with hot and cold thermal storages and hydrogen production. Renew Energy 2016/06/01/ 2016,;91:302–14. https://doi.org/10.1016/j.renene.2016.01.069.

[28] Cavalcanti EJC, Motta HP. Exergoeconomic analysis of a solar-powered/fuel assisted Rankine cycle for power generation. Energy 2015/08/01/ 2015,;88: 555–62. https://doi.org/10.1016/j.energy.2015.05.081.
[29] Wang J, Yan Z, Wang M, Ma S, Dai Y. Thermodynamic analysis and optimization of an (organic Rankine cycle) ORC using low grade heat source. Energy 2013/01/01/ 2013,;49:356–65. https://doi.org/10.1016/j.energy.2012.11.009.
[30] Auracher H. "Thermal design and optimization: Adrian Bejan, George Tsatsaronis and Michael Moran," ed: John Wiley & Sons Inc. NJ: Hoboken; 1996.
[31] Taheri MH, Mosaffa AH, Farshi LG. Energy, exergy and economic assessments of a novel integrated biomass based multigeneration energy system with hydrogen production and LNG regasification cycle. Energy 2017/04/15/ 2017,;125:162–77. https://doi.org/10.1016/j.energy.2017.02.124.
[32] Husebye J, Brunsvold AL, Roussanaly S, Zhang X. Techno Economic Evaluation of Amine based CO2 Capture: Impact of CO2 Concentration and Steam Supply. Energy Procedia 2012/01/01/ 2012,;23:381–90. https://doi.org/10.1016/j.egypro.2012.06.053.
[33] A. Buswell and W. Hatfield, "Anaerobic fermentations, state of Illinois," *Urbana, Illinois: Department of Registration and Education, Division of the State Wate r Survey,* 1936.
[34] Wellinger A, Murphy JP, Baxter D. The biogas handbook: science, production and applications. Elsevier; 2013.
[35] Yari M, Mehr AS, Mahmoudi SMS, Santarelli M. A comparative study of two SOFC based cogeneration systems fed by municipal solid waste by means of either the gasifier or digester. Energy 2016/11/01/ 2016,;114:586–602. https://doi.org/10.1016/j.energy.2016.08.035.
[36] Barati MR, et al. Comprehensive exergy analysis of a gas engine-equipped anaerobic digestion plant producing electricity and biofertilizer from organic fraction of municipal solid waste. Energ Conver Manage 2017/11/01/ 2017,;151: 753–63. https://doi.org/10.1016/j.enconman.2017.09.017.
[37] Hosseini SE, Barzegaravval H, Wahid MA, Ganjehkaviri A, Sies MM. Thermodynamic assessment of integrated biogas-based micro-power generation system. Energ Conver Manage 2016/11/15/ 2016,;128:104–19. https://doi.org/10.1016/j.enconman.2016.09.064.
[38] Zhang M, Chen H, Zoghi M, Habibi H. Comparison between biogas and pure methane as the fuel of a polygeneration system including a regenerative gas turbine cycle and partial cooling supercritical CO2 Brayton cycle: 4E analysis and tri-objective optimization. Energy 2022/10/15/ 2022,;257:124695. https://doi.org/10.1016/j.energy.2022.124695.
[39] Loha C, Chatterjee PK, Chattopadhyay H. Performance of fluidized bed steam gasification of biomass – Modeling and experiment. Energ Conver Manage 2011/03/01/ 2011,;52(3):1583–8. https://doi.org/10.1016/j.enconman.2010.11.003.
[40] Basu P. Biomass gasification, pyrolysis and torrefaction: practical design and theory. Academic press; 2018.
[41] Habibollahzade A, Ahmadi P, Rosen MA. Biomass gasification using various gasification agents: Optimum feedstock selection, detailed numerical analyses and tri-objective grey wolf optimization. J Clean Prod 2021/02/15/ 2021,;284: 124718. https://doi.org/10.1016/j.jclepro.2020.124718.
[42] Shayan E, Zare V, Mirzaee I. Hydrogen production from biomass gasification; a theoretical comparison of using different gasification agents. Energ Conver Manage 2018/03/01/ 2018,;159:30–41. https://doi.org/10.1016/j.enconman.2017.12.096.
[43] Asgari N, Khoshbakhti Saray R, Mirmasoumi S. Energy and exergy analyses of a novel seasonal CCHP system driven by a gas turbine integrated with a biomass gasification unit and a LiBr-water absorption chiller. Energ Conver Manage 2020/09/15/ 2020,;220:113096. https://doi.org/10.1016/j.enconman.2020.113096.
[44] Moran MJ, Shapiro HN, Boettner DD, Bailey MB. Fundamentals of engineering thermodynamics. John Wiley & Sons; 2010.
[45] Budisulistyo D, Krumdieck S. Thermodynamic and economic analysis for the pre-feasibility study of a binary geothermal power plant. Energ Conver Manage 2015/10/01/ 2015,;103:639–49. https://doi.org/10.1016/j.enconman.2015.06.069.
[46] Salek F, Moghaddam AN, Naserian MM. Thermodynamic analysis and improvement of a novel solar driven atmospheric water generator. Energ Conver Manage 2018/04/01/ 2018,;161:104–11. https://doi.org/10.1016/j.enconman.2018.01.066.
[47] Morosuk T, Tsatsaronis G. A new approach to the exergy analysis of absorption refrigeration machines. Energy 2008/06/01/ 2008,;33(6):890–907. https://doi.org/10.1016/j.energy.2007.09.012.
[48] Kim H, Rao SR, LaPotin A, Lee S, Wang EN. Thermodynamic analysis and optimization of adsorption-based atmospheric water harvesting. Int J Heat Mass Transf 2020/11/01/ 2020,;161:120253. https://doi.org/10.1016/j.ijheatmasstransfer.2020.120253.
[49] Mohammadpourfard M, Hajimohammadi Tabriz Z, Khani L. Design and Assessment of A New Dual Solid Oxide Fuel Cell – Gas Turbine Hybrid System. (in en), J Energy Managem Technol 2022. https://doi.org/10.22109/jemt.2022.329698.1372.
[50] Musharavati F, Khoshnevisan A, Alirahmi SM, Ahmadi P, Khanmohammadi S. Multi-objective optimization of a biomass gasification to generate electricity and desalinated water using Grey Wolf Optimizer and artificial neural network. Chemosphere 2022/01/01/ 2022,;287:131980. https://doi.org/10.1016/j.chemosphere.2021.131980.
[51] Darabadi Zare AA, Yari M, Nami H, Mohammadkhani F. Thermodynamic and thermoeconomic assessment of hydrogen production employing an efficient multigeneration system based on rich fuel combustion. Int J Hydrogen Energy 2023/03/26/ 2023,;48(26):9861–80. https://doi.org/10.1016/j.ijhydene.2022.11.296.
[52] Freund D, Güngör A, Atakan B. "Hydrogen production and separation in fuel-rich operated HCCI engine polygeneration systems: Exergoeconomic analysis and comparison between pressure swing adsorption and palladium membrane separation," *Applications in Energy and Combustion.* Science 2023/03/01/ 2023,;13: 100108. https://doi.org/10.1016/j.jaecs.2022.100108.
[53] "CEPCI." https://www.chemengonline.com/2023-cepci-updates-january-prelim-and-december-2022-final/ (accessed.
[54] Zare AAD, Yari M, Mohammadkhani F, Nami H, Desideri U. Thermodynamic and exergoeconomic analysis of a multi-generation gas-to-X system based on fuel-rich combustion to produce power, hydrogen, steam and heat. Sustain Cities Soc 2022/11/01/ 2022,;86:104139. https://doi.org/10.1016/j.scs.2022.104139.
[55] M. H. Taheri, L. Khani, M. Mohammadpourfard, H. Aminfar, and G. G. Akkurt, "Multi-objective optimization of a novel supercritical CO2 cycle-based combined cycle for solar power tower plants integrated with SOFC and LNG cold energy and regasification," *International Journal of Energy Research,* https://doi.org/10.1002/er.7972 vol. 46, no. 9, pp. 12082-12107, 2022/07/01 2022, doi: https://doi.org/10.1002/er.7972.
[56] Balafkandeh S, Zare V, Gholamian E. Multi-objective optimization of a tri-generation system based on biomass gasification/digestion combined with S-CO2 cycle and absorption chiller. Energ Conver Manage 2019/11/15/ 2019,;200: 112057. https://doi.org/10.1016/j.enconman.2019.112057.
[57] Ahmadi P, Dincer I, Rosen MA. Thermoeconomic multi-objective optimization of a novel biomass-based integrated energy system. Energy 2014/04/15/ 2014,;68: 958–70. https://doi.org/10.1016/j.energy.2014.01.085.
[58] Liu Z, Ehyaei MA. Thermoeconomic and exergoenvironmental assessments of a combined micro-gas turbine and superheated Kalina cycles for cogeneration of heat and electrical power using biomass. Int J Environ Sci Technol 2022/11/01 2022,;19(11):11233–48. https://doi.org/10.1007/s13762-022-04329-y.
[59] Akrami E, Chitsaz A, Nami H, Mahmoudi SMS. Energetic and exergoeconomic assessment of a multi-generation energy system based on indirect use of geothermal energy. Energy 2017/04/01/ 2017,;124:625–39. https://doi.org/10.1016/j.energy.2017.02.006.
[60] Talebizadehsardari P, et al. Energy, exergy, economic, exergoeconomic, and exergoenvironmental (5E) analyses of a triple cycle with carbon capture. J CO2 Util 2020/10/01/ 2020,;41:101258. https://doi.org/10.1016/j.jcou.2020.101258.
[61] Ji-chao Y, Sobhani B. Integration of biomass gasification with a supercritical CO2 and Kalina cycles in a combined heating and power system: A thermodynamic and exergoeconomic analysis. Energy 2021/05/01/ 2021,;222:119980. https://doi.org/10.1016/j.energy.2021.119980.
[62] A. Baghernejad and M. Yaghoubi, "Multi-objective exergoeconomic optimization of an Integrated Solar Combined Cycle System using evolutionary algorithms," *International Journal of Energy Research,* https://doi.org/10.1002/er.1715 vol. 35, no. 7, pp. 601-615, 2011/06/10 2011, doi: https://doi.org/10.1002/er.1715.
[63] Ahmadi P, Dincer I. 1.8 Exergoeconomics. Comprehensive energy systems 2018;1: 340–76.
[64] Khani L, Mahmoudi SMS, Chitsaz A, Rosen MA. Energy and exergoeconomic evaluation of a new power/cooling cogeneration system based on a solid oxide fuel cell. Energy 2016/01/01/ 2016,;94:64–77. https://doi.org/10.1016/j.energy.2015.11.001.
[65] Behzadi A, Gholamian E, Houshfar E, Habibollahzade A. Multi-objective optimization and exergoeconomic analysis of waste heat recovery from Tehran's waste-to-energy plant integrated with an ORC unit. Energy 2018/10/01/ 2018,;160:1055–68. https://doi.org/10.1016/j.energy.2018.07.074.
[66] Ehyaei MA, Baloochzadeh S, Ahmadi A, Abanades S. Energy, exergy, economic, exergoenvironmental, and environmental analyses of a multigeneration system to produce electricity, cooling, potable water, hydrogen and sodium-hypochlorite. Desalination 2021/04/01/ 2021,;501:114902. https://doi.org/10.1016/j.desal.2020.114902.
[67] Adewusi SA, Zubair SM. Second law based thermodynamic analysis of ammonia–water absorption systems. Energ Conver Manage 2004/09/01/ 2004,;45 (15):2355–69. https://doi.org/10.1016/j.enconman.2003.11.020.
[68] "Çiğli Climate." https://climate.onebuilding.org/WMO_Region_6_Europe/TUR_Turkey/index.html#IDIZ_Izmir (accessed.
[69] "Cigli." https://www.izsu.gov.tr/tr/TesisDetay/1/80/1?AspxAutoDetectCookieSupport=1 (accessed.
[70] Cartmell E, et al. BiosolidsA Fuel or a Waste? An Integrated Appraisal of Five Co-combustion Scenarios with Policy Analysis. Environ Sci Tech 2006/02/01 2006,;40 (3):649–58. https://doi.org/10.1021/es052181g.
[71] Shayan E, Zare V, Mirzaee I. Exergoeconomic Analysis of an Integrated Steam Biomass Gasification System with a Solid Oxide Fuel Cell for Power and Freshwater Generations [Online]. Available: mdrsjrns 2020;20(3):553–64. http://mme.modares.ac.ir/article-15-27327-en.html.
[72] Walraven D, Laenen B, W. D'haeseleer,. Minimizing the levelized cost of electricity production from low-temperature geothermal heat sources with ORCs: Water or air cooled? Appl Energy 2015/03/15/ 2015,;142:144–53. https://doi.org/10.1016/j.apenergy.2014.12.078.